

Investigation of the role of the phenylpropanoid pathway and cell wall fortification in the inhibitory effect of plant basal resistance on bacteria

OTKA/NKFIH PD 109050

Objectives of the project

Plant basal resistance (BR), or in other words pattern triggered immunity (PTI) is a symptomless form of plant resistance that lets plants to detect and block a diverse set of microorganisms. PTI can be triggered by microbe associated molecular patterns (MAMPS), such as the conserved Flg22 peptide of bacterial flagellin, elongation factor Tu (EF-Tu), peptidoglycan (PGN), lipopolysaccharides (LPS), Ax21 (Activator of XA21-mediated immunity in rice) (reviewed in: Newman et al. 2013). PTI is effective against a broad range of microbes. Its early signaling events include rapid calcium influx, production of reactive oxygen species (ROS) and mitogen activated protein kinase (MAPK) phosphorylation cascades which then lead to callose deposition, and defense gene expression presumably mediating inhibition of microbial growth (Withers and Dong, 2017).

During our previous work we identified over 400 EST-s representing 176 individual genes that are activated during PTI. Phenylpropanoid genes were highly represented, and covered a major part of the currently known network of the phenylpropanoid pathway. Our hypothesis was that the phenylpropanoid pathway might play an important role in the inhibitory effects of PTI on bacteria, either by leading to cell wall fortification or by some phenolic compounds having direct antimicrobial effect, or else, by acting as a signalling agent, affecting virulence factors of bacteria.

Some MYB transcription factors have been proposed to regulate plant defence responses by enhancing phenylpropanoid metabolism in response to fungal MAMPS. Kishi-Kaboshi et al (2018) identified three MYB proteins that were transcriptionally induced by fungal MAMP treatment. Induced expression of these MYB genes systematically and specifically induced a large part of the genes encoding enzymes in the cinnamate/monolignol pathway. However, to our knowledge, they have not been investigated in relation to bacterially induced PTI prior to the starting time of this project. An interesting study of Chezem and co-workers was published in 2017. They showed that *Arabidopsis thaliana* myb15 and lignin biosynthetic mutants showed increased susceptibility to the bacterial pathogen *Pseudomonas syringae*, supporting defence-induced lignin having a major role in basal immunity. Consistent with our hypothesis based on tobacco derived data, they claimed their results supported a role for phenylalanine-derived small molecules in preformed and inducible *Arabidopsis* defence, a role previously dominated by tryptophan-derived small molecules.

Our main goals were to find out if silencing, or overexpression of PTI-related phenylpropanoid and MYB transcription factor genes, or pharmacological inhibition of the corresponding enzymes leads to significant alterations in the efficiency of PTI. We also aimed at tracking changes in metabolite levels corresponding PTI and consider these changes as markers of PTI, or possibly test for direct or indirect antimicrobial activities of some of the identified compounds.

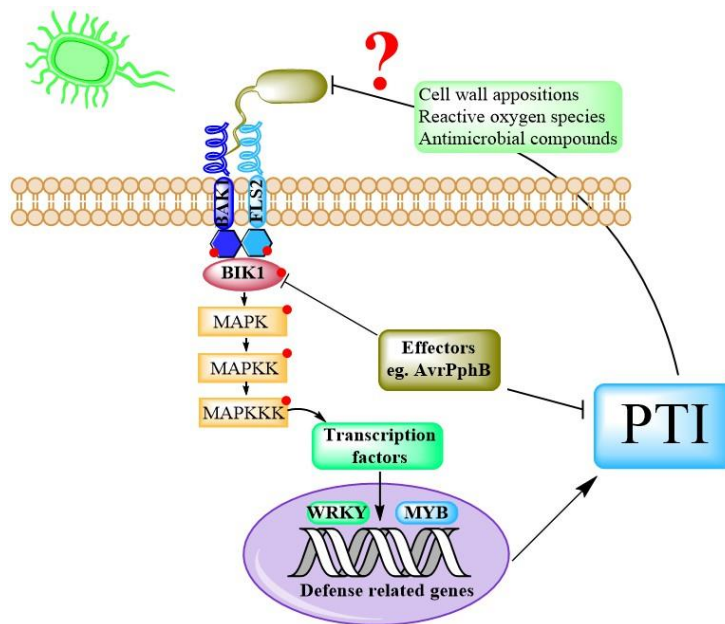


Fig. 1. Mechanism of PAMP triggered immunity (PTI). Recognition of pathogen/microbe associated molecular patterns (PAMP) by plant pattern recognition receptors like FLS2 induces signaling involving mitogen associated protein kinase (MAPK) cascades, resulting in activation of transcription factors, nuclear gene induction and eventually basal resistance in the infected tissue. This type of immunity is termed PAMP triggered immunity or PTI. Pathogen derived effectors including avirulence proteins (Avr) can interfere with PTI. (based on Chisholm et al. 2006, Withers and Dong 2017, Kachroo et al. 2017)

Silencing of phenylpropanoid and MYB transcription factor genes related to PTI

For virus induced gene silencing (VIGS) of PTI-related phenylpropanoid genes and MYB transcription factors, we chose a modified version of the Tobacco Rattle Virus - Phytoene Desaturase (TRV-PDS) vector: the TRV - Green Fluorescent Protein (TRV-GFP), that uses co-silencing of GFP in *N. benthamiana* or *Arabidopsis* plants constitutively expressing GFP to report successful silencing of the gene of interest (Fig. 2., Fodor et al. 2018, Ramegowda et al. 2013).

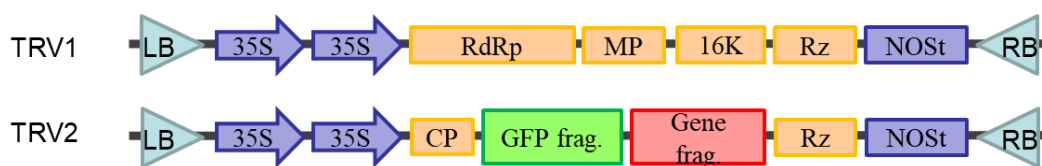


Fig. 2. Map of Tobacco Rattle Virus (TRV) based VIGS vectors that enable visual detection of successful silencing

Five PTI-related *N. tabacum* phenylpropanoid genes were selected, based on our former suppression subtractive hybridization studies (Szatmári et al. 2014).

- PAL c64; phenilalanine ammonia-lyase
- C4H c45; cinnamate 4-hydroxylase
- 4CL c51; 4-hydroxycinnamoyl-CoA ligase
- OMTI c1; O-methyltransferase
- F5H c39; ferulate 5-hydroxylase

We selected four MYB factors for silencing:

- NtMYB35
- NtMYB48
- NtMYBGR1
- NtMYB2

NtMYB2 and MYBGR1 are known from literature (Shinya 2007, Sugimoto et al. 2000) to be induced by fungal MAMPS. We have shown that NtMYB35 and NtMYB48 genes are repressed, while MYBGR1 was found to be activated by *Pseudomonas* bacteria during PTI (results published in Bozsó et al. 2016).

First we used NCBI Blast and Sol Genomics Network Blast engine (<https://solgenomics.net>) to identify the closest *N. benthamiana* homologs of the selected *N. tabacum* genes. The Sol Genomics VIGS Tool was then used to choose the best target regions for VIGS of the selected gene, and its closest homologs as well, because we were aiming to silence not only gene activities, but also the corresponding enzymatic activities.

Constructs containing a shorter (cca. 300 bp) and a longer (cca. 600 bp) insert from *N. benthamiana* C4H (cinnamate 4-hydroxylase) and MYBGR1 transcription factor genes were cloned into the TRV2-GFP vector, then were transformed into *Agrobacterium tumefaciens* and were used to inoculate *N. benthamiana* leaves. This part of the work contributed to publication of a technical article on the improvement of transformation efficiency of *Agrobacterium* by electroporation (Kámán-Tóth et al. 2018).

Then, gene silencing efficiency of the above four constructs was tested. Visual evaluation was possible by detecting disappearance of green fluorescence. Supposedly, co-silencing of the required gene would also occur, as TRV2 contained the fragments of GFP and the gene in tandem. GFP silencing was visible with each construct. The silencing efficiency of shorter and longer inserts was compared as a first step. Longer constructs generally result in more efficient VIGS, however, virus replication might be reduced if they are too long. Maximal insert length was not known in case of the TRV-GFP vector.



Fig. 3. Example of detection of gene silencing using GFP co-silencing. The control *N. benthamiana* plant expressed GFP constitutively.

Real-time PCR was used to quantitate silencing efficiency. PTI was induced in silenced leaves by *Pseudomonas syringae* pv. *syringae hrcC-* (HR deficient) bacteria. Leaf samples were taken 3 hours later for RNA extraction, DNase treatment, and cDNA generation. Real-time PCR was carried out using MYBGR1 and C4H specific primers, and ubiquitine (UBI) as constitutive control. PTI-induced activation of C4H was silenced effectively in both constructs, by -90-97% as compared to the GFP control. Silencing of MYBGR1 was -50-60% in the 622 bp construct and no significant silencing was detected in case of the 300 bp construct.

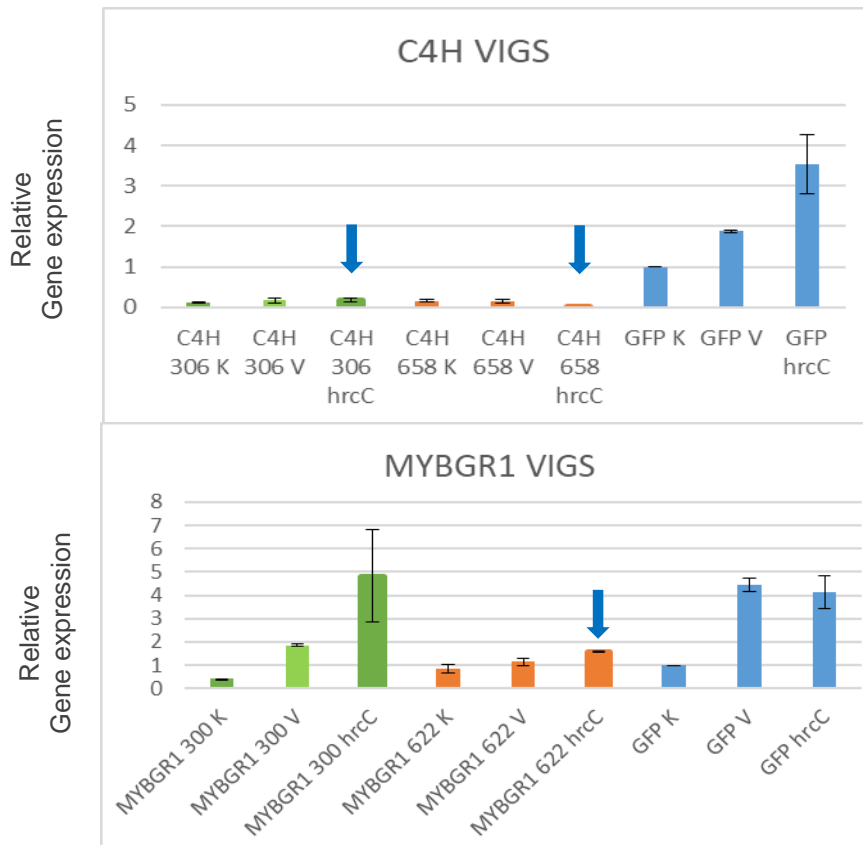


Fig. 4. Evaluation of effective gene silencing of C4H and MYBGR1 in PTI induced *N. benthamiana* plants (3 hpi). Significant difference of hrcC induced VIGS plant form hrcC induced GFP control calculated with student's t-test is marked by a blue arrow ($p < 0.05$). K: non-treated control. V: water injected control. hrcC: inoculation with *P. syringae* pv. *syringae* hrcC- (HR-negative) bacteria – PTI-inducing strain.

Based on these results, the TRV2-GFP constructs with longer (cca. 600 bp) inserts were expected to perform more reliably, so the further silencing constructs were designed with long inserts for the following genes: Phenylalanine Ammonia Lyase (PAL), 4-coumarate-Coenzyme A ligase (4CL), Caffeic acid O-methyltransferase 1 (COMT1), Ferulate-5-Hydroxylase (F5H), and transcription factors NtMYB2, MYB35 and MYB48.

Efficiency of silencing was again evaluated by real time RT-PCR in leaves inoculated with PTI-inducing *Pseudomonas syringae* pv. *syringae* hrcC- bacteria. This was necessary, because some genes had low basal transcription levels, so their silencing was only detectable, when they were induced. VIGS efficiency was also observed visually by detecting disappearance of green fluorescence in GFP-expressing *N. benthamiana* leaves. Silencing of five genes proved to be sufficient (70-95%) in PTI-induced leaf samples (6 hpi) by real-time RT-PCR, compared to PTI-induced control plants silenced with the empty TRV-GFP vector (Fig. 5). Silencing of the two repressed transcription factors, MYB35 and MYB48 did not seem to add significant further transcriptional downregulation compared to the empty TRV-GFP vector.

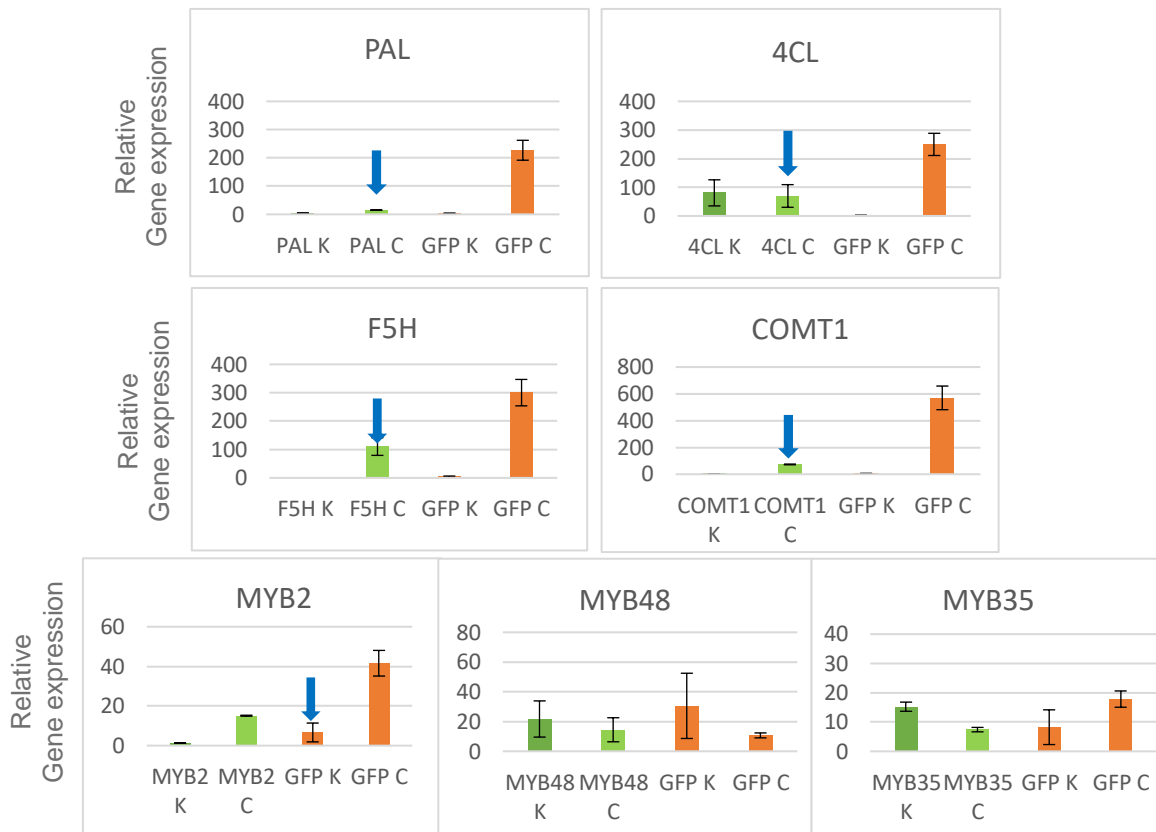


Fig. 5. Evaluation of effective gene silencing of Phenylalanine Ammonia Lyase (PAL), 4-coumarate-Coenzyme A ligase (4CL), Caffeic acid O-methyltransferase 1 (COMT1), Ferulate-5-Hydroxylase (F5H), and transcription factors NtMYB2, MYB35 and MYB48 in PTI induced *N. benthamiana* plants (6 hpi). Significant difference of hrcC induced VIGS plants form hrcC induced GFP control calculated with a student's t-test is marked by a blue arrow ($p < 0.05$). K: non-treated control. V: water injected control. C: inoculation with *P. syringae* pv. *syringae* hrcC- (HR-negative) bacteria – PTI-inducing strain.

One of the constructs had a strong phenotype: the newly developed leaves of the 4CL VIGS construct were small, dwarfed ones.

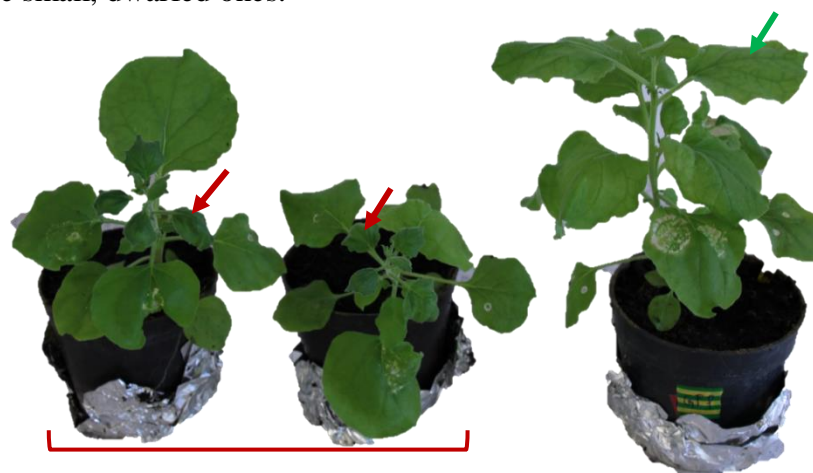


Fig. 6. 4CL-GFP-VIGS dwarfed upper leaves Control (GFP-VIGS)

To study the effects of silencing of phenylpropanoid and MYB genes on PTI, HR-inhibition tests were carried out. (This test utilizes the phenomenon that PTI normally inhibits the development of the HR.) Upper and middle leaves of silenced *N. benthamiana* plants were pre-

inoculated with *Pseudomonas syringae* pv. *syringae* *hrcC*- bacteria to induce PTI. 6 hours later overlapping areas were inoculated with incompatible *P. syringae* pv. *tomato* DC3000 suspension. Occurrence of HR was registered two days later.

Silencing of the MYBGR1 gene caused the most significant reduction in PTI, compared to GFP control leaves. NtMYB2 VIGS also caused significant reduction in PTI. The PAL, F5H and NtMYB2 VIGS constructs also reduced PTI efficiency significantly. C4H silencing resulted in reduced PTI, which was only significant, when challenge inoculation followed 4 hours after PTI induction. PTI efficiency was also reduced in COMT1 silenced leaves, but this was not significant at 6 hpi.

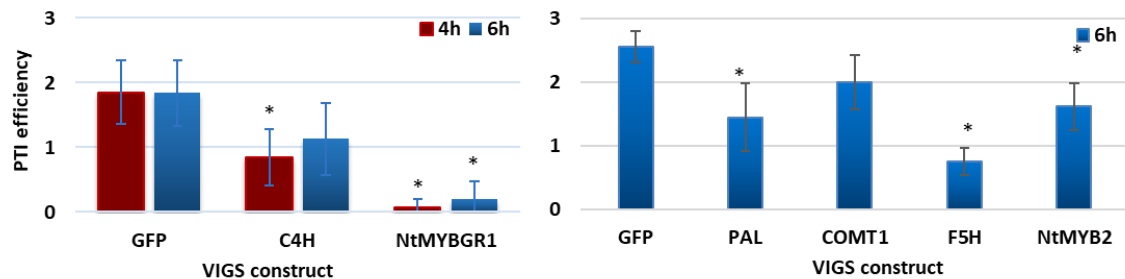


Fig. 7. Evaluation of PTI efficiency of plants transiently silenced in Phenylalanine Ammonia Lyase (PAL), Caffeic acid O-methyltransferase 1 (COMT1), Ferulate-5-Hydroxylase (F5H), and NtMYB2, and MYBGR1 transcription factor genes in PTI induced *N. benthamiana* plants. Preinoculation was carried out with *P. syringae* pv. *syringae* *hrcC*- (HR-negative) bacteria – PTI-inducing strain, then challenge inoculation with incompatible *P. syringae* pv. *tomato* DC3000 (A: 4 and 6 hpi; B: 6 hpi). Visual absence of HR scored 3, full HR scored 0, detected 48 hours after the challenge inoculation. Significant difference from GFP control according to student's *t*-test is marked by a * ($p < 0.05$).

Arabidopsis mutants

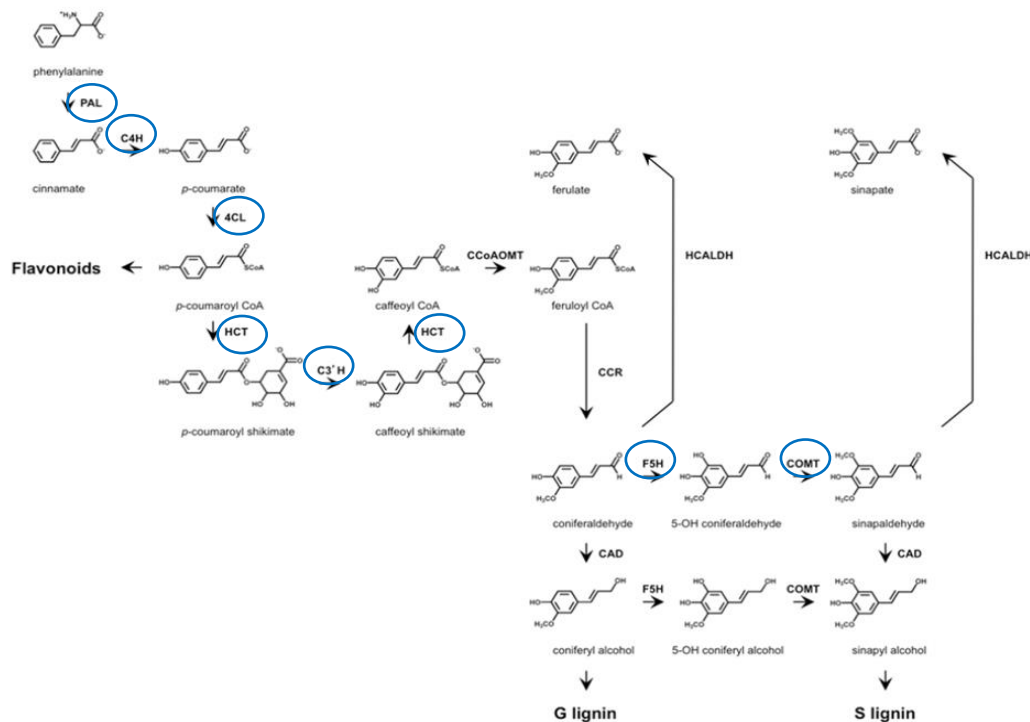


Fig. 8. Phenylpropanoid metabolism in *Arabidopsis*. Blue circles indicate genes whose T-DNA or ethylmethane sulfonate mutants were tested for decreased resistance. PAL, phenylalanine ammonia-

lyase; C4H, cinnamic acid 4-hydroxylase; 4CL, 4-coumarate:CoA ligase; HCT, hydroxycinnamoyl-coenzyme A shikimate:quinic acid hydroxycinnamoyl-transferase; C3'H, p-coumaroyl shikimate 3'-hydroxylase; CCoAOMT, caffeoyl CoA 3-O-methyltransferase; CCR, cinnamoyl-CoA reductase; F5H, ferulate 5-hydroxylase; COMT, caffeic acid/5-hydroxyferulic acid O-methyltransferase; CAD, cinnamyl alcohol dehydrogenase; HCALDH, hydroxycinnamaldehyde dehydrogenase. From: Fraser and Chapple 2011.

The core mechanism of PTI in *Arabidopsis* as a model plant from the *Brassicaceae* family is similar to that of tobacco and other members of the *Solanaceae* family, however it differs in several details. In order to find out if silencing of any phenylpropanoid genes results in similar changes of PTI efficiency in *Arabidopsis* as in *Nicotiana*, we decided to find *Arabidopsis* homologues of the genes silenced by VIGS. We ordered T-DNA and ethylmethane sulfonate mutants of these genes from NASC (Nottingham Arabidopsis Stock Centre).

T-DNA mutants are essentially different from VIGS plants as T-DNA mutants are normally mutated in a single gene of a gene family, while VIGS is able to repress transcription of redundant homologous genes. *Arabidopsis* eg. has four PAL and 4CL genes. These can have distinct roles, and not all of them are necessarily involved in PTI. For example 4CL1 accounts for the majority of the total 4CL activity in *Arabidopsis*, and 4CL1, 4CL2, and 4CL4 are more closely related to each other than to 4CL3, suggesting that the two groups may serve different biological functions. Promoter-GUS analysis showed that 4CL1 and 4CL2 are expressed in lignifying cells (Li et al. 2015). In the case of PAL, only quadruple mutants showed significantly enhanced disease susceptibility to *Pseudomonas syringae* pv. *tomato* DC3000, the individual homologues being greatly redundant in function (Huang et al. 2010). So, using SALK mutants, individual genes related to PTI can be selected, while using VIGS, homologous genes can be silenced parallelly. Importantly, C4H in *Arabidopsis* is a single gene, and complete absence of it is lethal. The C4H mutant used here is a mismatch mutant, and the gene product has been shown to have reduced activity (Schilmiller et al. 2009).

The SALK mutants used in our experiments were selected based on homology to the silenced *Nicotiana* genes. Their transcriptional activation to PTI inducers was also confirmed using the Arabidopsis eFP Browser (http://bar.utoronto.ca/efp/cgi-bin/efpWeb.cgi?dataSource=Biotic_Stress). The following mutants were tested:

Gene	NASC ID	SALK ID
PAL1	N656265	SALK_022804C
PAL2	N661248	SALK_000357C
C4H	N66576	ref3-3
4CL1	N675469	SALK_061752C
4CL2	N677245	SALK_143754C
4CL3	N671432	SALK_057020C
4CL4	N655576	SALK_063824C
OMT1	N25167	SALK_135290
OMT2	N681044	SALK_020611C
C3H1	N678975	SALK_112823C
C3H2	N667822	SALK_014048C
HCT	N698890	SALK_061912C
AtMYB1	N694605	SALK_205432C
AtMYB2	N690642	SALK_202624C
AtMYB2	N660266	SALK_151976C
AtMYB4	N665419	SALK_018565C

P. syringae pv *tomato* DC3000 (Pst DC3000) infection assay of wild-type *Arabidopsis* and T-DNA mutants was carried out to assess if downregulation of any of these genes leads to significant reduction in the ability of compatible bacteria to proliferate *in vivo*. Six leaves of 6-9 plants per mutant were syringe infiltrated with 10^5 CFU/ml suspension of bacteria grown overnight. Leaf samples were taken 3 days later with cork a borer, bacteria were re-isolated in 0.5 ml 10mM $MgCl_2$ solution and serial dilutions were spread on to King's B agar plates. Bacterial counts were determined after 2 days of incubation.

Pst DC3000 bacteria proliferated significantly faster in three SALK mutants than in the wild type Col0. These were a C4H (cinnamic acid 4-hydroxylase), a C3H (p-coumaroyl shikimate 3'-hydroxylase), and a 4CL (4-coumarate:CoA ligase) mutant (Fig. 9). The difference was most pronounced in the C4H mutant. This result indicates that metabolite(s) synthesised downstream of these enzymes in the *Arabidopsis* phenylpropanoid pathway might play an important role in resistance against compatible Pst DC3000.

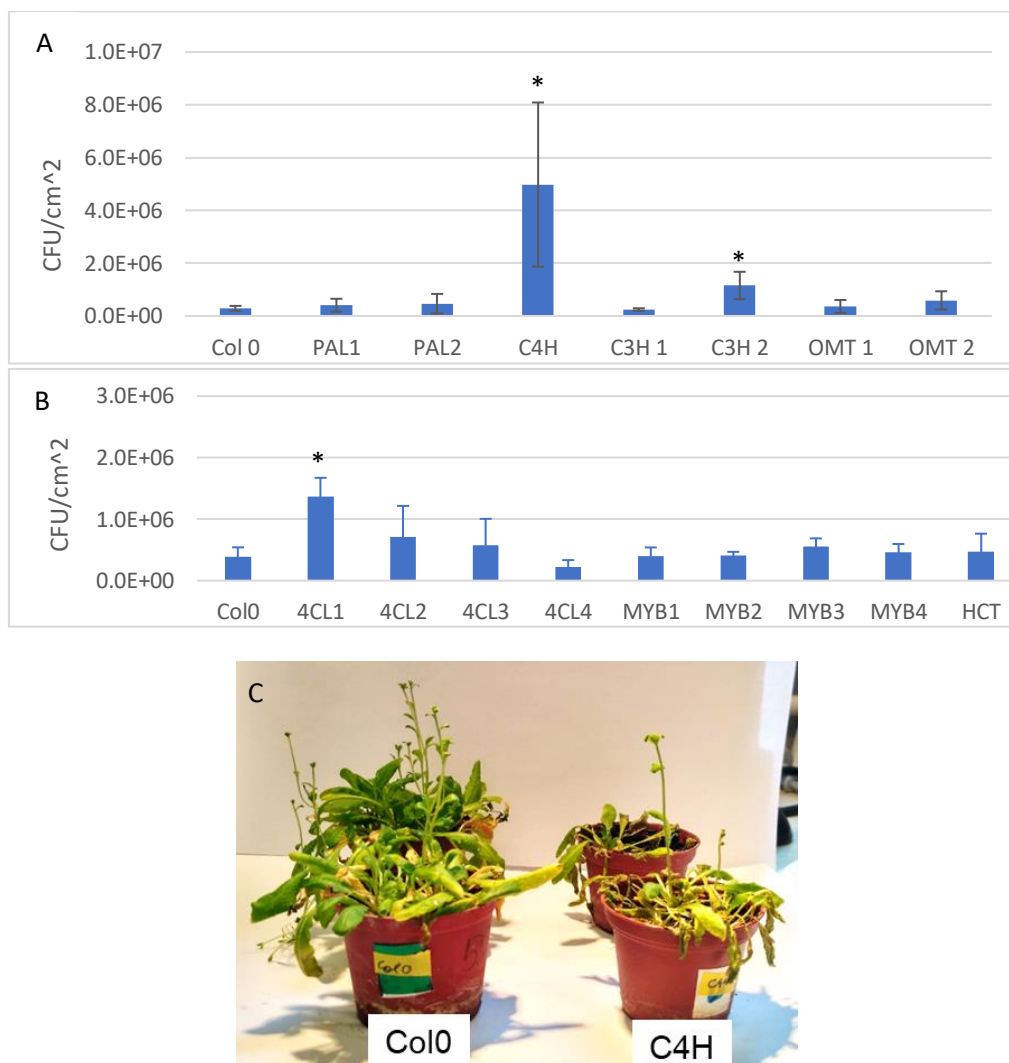


Fig. 9. A) and B) Proliferation of compatible *Pseudomonas syringae* pv. *tomato* DC3000 bacteria (10^5 CFU/ml inoculum) in different *Arabidopsis* SALK mutants. Phenylpropanoid and MYB gene mutants were selected based on homology with PTI-induced tobacco genes. Samples for bacterial counts were taken 3 dpi. Significant difference from wild type Col0 according to student's *t*-test is marked by a * ($p < 0.05$). C) Difference in visible symptoms on C4H mutant and Col0 control plants 6 dpi. Abbreviations: Col0, control line, PAL, phenylalanine ammonia-lyase; C4H, cinnamic acid 4-hydroxylase; 4CL, 4-coumarate:CoA ligase; HCT, hydroxycinnamoyl-coenzyme A shikimate:quinase

hydroxycinnamoyl-transferase; C3H, p-coumaroyl shikimate 3'-hydroxylase; F5H, ferulate 5-hydroxylase; COMT, caffeic acid/5-hydroxyferulic acid O-methyltransferase.

Overexpression

For transient overexpression studies, the same PTI-related *N. tabacum* phenylpropanoid genes were selected as for silencing: PAL; C4H; 4CL; OMT1b and F5H. MYB transcription factors were also the same: NtMYB35-1; NtMYBGR1; NtMYB48-1 and NtMYB2 along with a GFP gene as control.

Full *Nicotiana tabacum* CDS sequences of all corresponding genes have been obtained from GenBank, and primers were designed to clone full ORFs into the pEarleyGate 100 binary gateway vector. 11 different full length ORFs were cloned into the pDONR/ZEO vector. Sequencing revealed that besides the original genes, variants of these phenylpropanoid and MYB genes were also cloned.

The following full ORFs were obtained:

1. C4H (cinnamate 4-hydroxylase)
2. 4CL (4-hydroxycinnamoyl-CoA ligase)
3. OMT1b (O-methyltransferase)
4. OMT1bv (O-methyltransferase variant)
5. PAL (phenylalanine ammonia-lyase)
6. F5H (ferulate 5-hydroxylase)
7. MYBGR1 transcription factor
8. MYBGR1v - MYBGR1 transcription factor variant
9. eGFP ER (Enhanced GFP, endoplasmic reticulum-targeted) Strong green fluorescence obtained when using the construct.

From among the planned MYB constructs, only the cloning of MYBGR1 gene was successful, despite us taking great effort to obtain the other ones as well. A MYB related 306 like (MYBrel 306L) was cloned unintendedly, with the primers designed for NtMYB35. MYB35 and MYBrel 306L are highly homologous, with 91.63% overall sequence identity, but nearly 100% at the 5' and 3' ends. Difficulty with cloning full ORFs of MYB transcription factors might be due to the low relative abundance of MYB factor transcripts in plant cells, and the presence of highly homologous genes in this abundant gene family.

Verification of transient overexpression

The cloned ORFs from pDONR intermedier plasmids were inserted into the binary vector pEarleyGate 100, then transformed into *A. tumefaciens* used to infiltrate *N. benthamiana* leaves. 3 days later leaf samples were taken for RNA extraction, and cDNA generation. Overexpression was then tested by real-time PCR, with gene-specific primers. Transient overexpression of each gene was verified, in the range of 10-fold to 200-fold, as compared to the control plants transformed with an empty PE100 vector (Fig. 10).

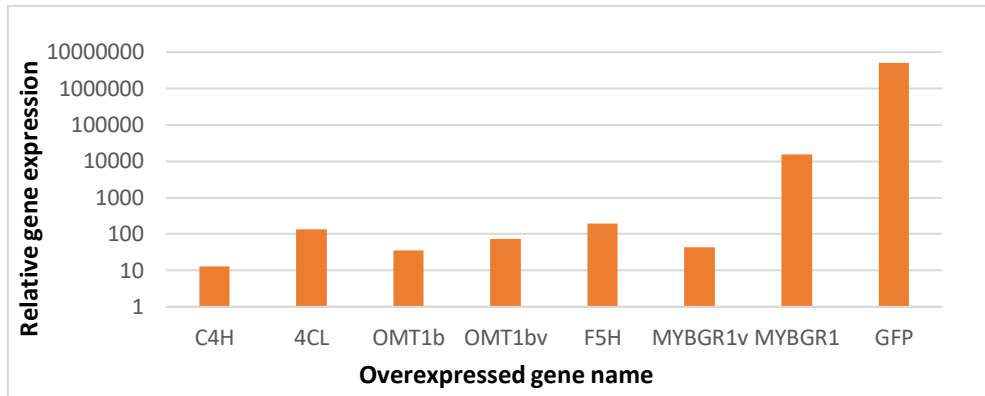


Fig. 10. Confirmation of transient overexpression of phenylpropanoid genes and MYB transcription factors in *N. benthamiana* by real time RT-PCR. Samples were taken 3 days after infections with *Agrobacteria* containing the specific *PEarleygate100* binary vector constructs. Data were normalized with values from the empty-vector construct. GFP: green fluorescent protein, C4H - cinnamic acid 4-hydroxylase, 4CL - 4-coumarate:coenzyme A ligase, OMT1b and OMT1bv - Orthomethyltransferase I-b and a variant, F5H - ferulate-5-hydroxylase, MYBGR1: transcription factor.

Testing for signs of altered PTI development (Fig. 11). To test whether any of the overexpressed genes was able to affect the proliferation of compatible pathogenic bacteria in planta, *Pseudomonas syringae* pv. *tabaci* (*P. tabaci*) was injected into overexpressing *N. benthamiana* leaves. Samples were taken at 0, 1 and 3 dpi. Proliferation of *P. tabaci* was detected by real-time PCR, because of the presence of *Agrobacteria*. A *Pseudomonas* specific primer pair (verified not to amplify any *Agrobacterium* sequences) was used. As an alternative method to monitor the effect of overexpression on PTI we transformed the pDSK-GFPuv plasmid into *P. tabaci* to gain fluorescent compatible bacteria that can be visually discriminated from *Agrobacteria*. Proliferation of the fluorescent bacteria was determined by re-isolation from leaves and serial dilutions for CFU determination on agar plates.

At 3 dpi, the relative quantity of *P. tabaci* in C4H, 4CL, OMT1b and F5H overexpressing leaves was significantly lower than in GFP expressing vector controls as detected by real time RT-PCR. Similar results were obtained with bacterial CFU counting, except 4CL not showing significant difference in this case. MYBGR1 overexpression did not influence *P. tabaci* proliferation, moreover, the MYBGR1 even enhanced pathogen growth.

Of the two detection methods, eventually RT-PCR seemed to be a more accurate to measure bacterial growth rate, however CFU counting might also provide important data, as it gives information about truly viable and culturable bacteria.

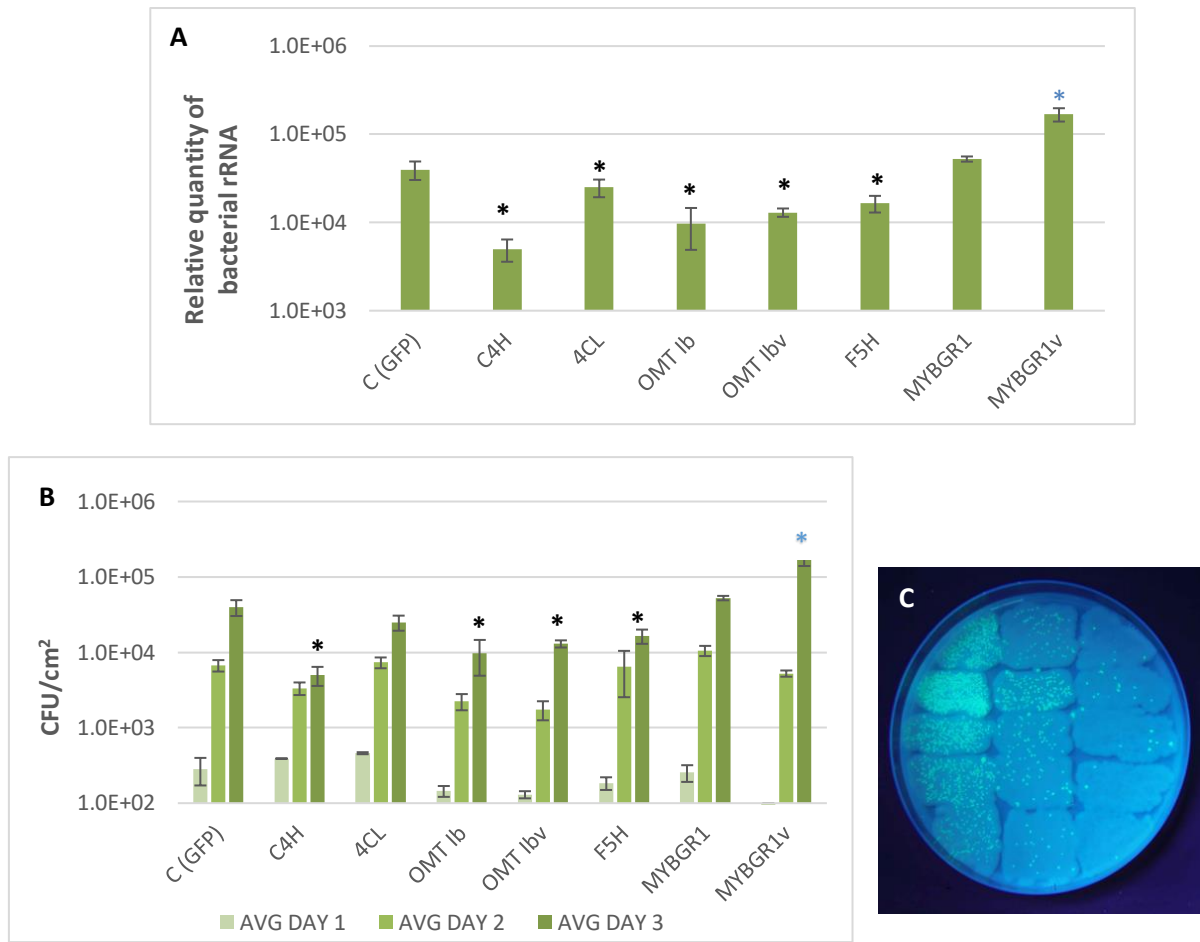


Fig. 11. Proliferation of *P. tabaci* in phenylpropanoid gene-overexpressing *N. benthamiana* leaves. A) Proliferation of *Pseudomonas syringae* pv. *tabaci* bacterium determined 3 dpi with RT-PCR using a *Pseudomonas*-specific primer pair. B) Fluorescent *P. tabaci* bacteria harbouring a *pDSK-GFPuv* plasmid were re-isolated from plant leaves for CFU determination. C) Proliferation of *P. tabaci* bacteria determined by re-isolation from leaves, and serial dilutions. Significant difference from GFP control according to student's *t*-test is marked by a * ($p < 0.05$).

Pharmacological inhibition

To support possible results from silencing experiments, we selected pharmacological inhibitors of phenylpropanoid enzymes, such as piperonylic acid (PIP), a selective, quasi-irreversible inhibitor of C4H investigated earlier (Szatmári et al. 2014). We tested aminooxyacetic acid (AOAA) known to inhibit phenylalanine ammonia-lyase (PAL), 3,4-methylenedioxycinnamic acid (MDCA) that inhibits 4-coumarate-CoA ligase (4CL), and a competitive inhibitor of F5H is 5-hydroxyconiferyl aldehyde (ConAld), although this inhibition has only been shown in vitro.

To test the effect of pharmacological inhibition of selected phenylpropanoid enzymes on BR development, HR-inhibition tests were carried out on *N. tabacum* plants using pre-inoculations of *Pseudomonas syringae* pv. *syringae hrcC*- (PTI inducing), and challenge inoculations of *Pseudomonas syringae* pv. *syringae* 61 (incompatible, HR inducing). Piperonylic acid (PIP; C4H inhibitor), aminooxyacetic acid (AOAA; PAL inhibitor), 3,4-methylenedioxycinnamic acid (MDCA, 4CL inhibitor) and coniferyl aldehyde (CONAL, F5H inhibitor) were injected either alone, or in combination with *P. syringae* pv. *syringae hrcC*- suspension. The infiltrated area was circumscribed, and 6 hours later the challenging incompatible bacteria were injected to the same area.

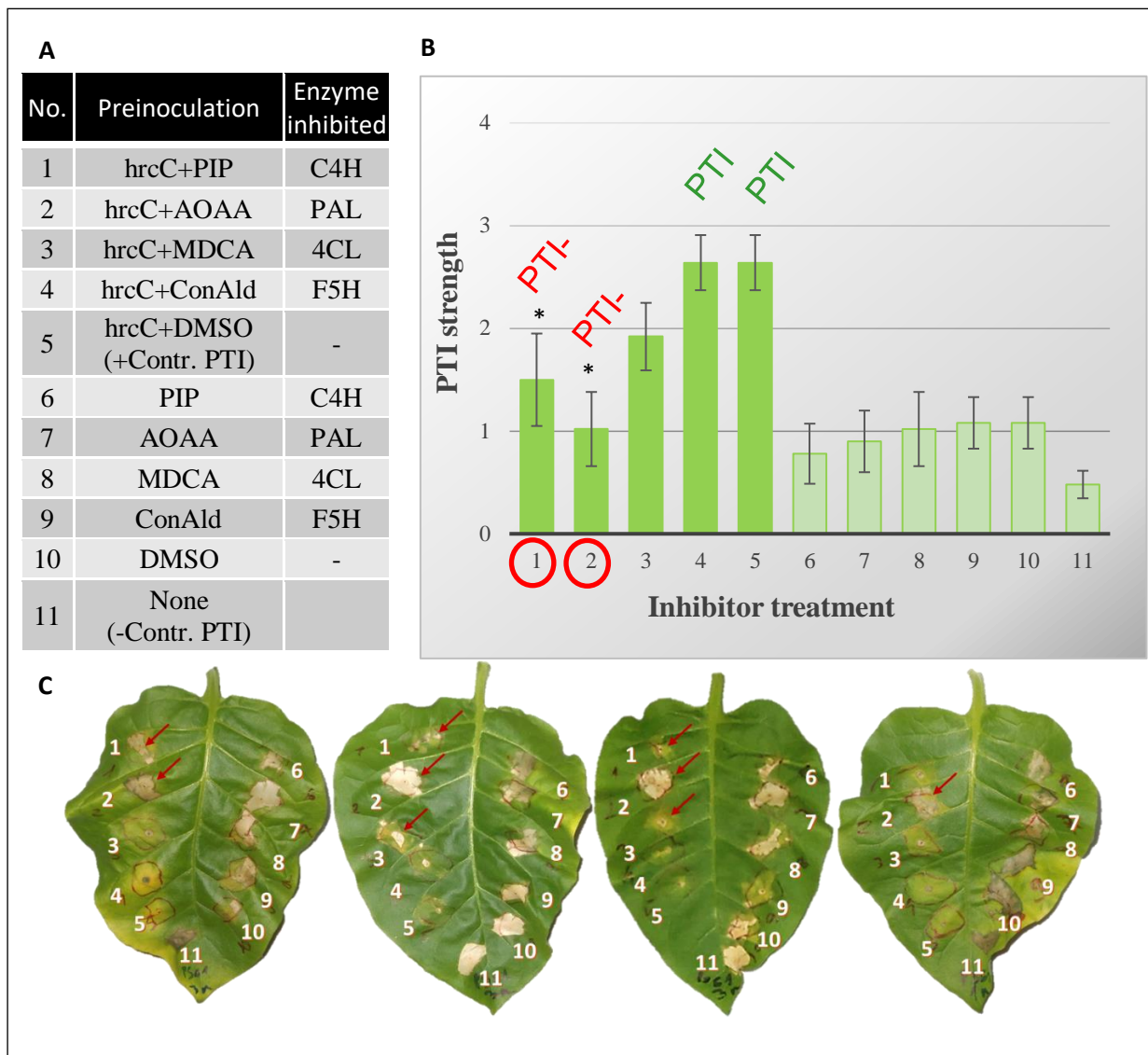


Fig. 12. Pharmacological inhibition of phenylpropanoid enzymes affects PTI efficiency in *N. tabacum*, as revealed by HR-test. A) Pre-inoculations in interveinal regions of *N. tabacum* leaves were done as denoted in the table, followed by challenge inoculation with incompatible *P. syringae* pv. *syringae* 61 bacterial suspension 6 hours later. Strength of HR was scored 2 days later. 1-4 test treatments. 5 PTI positive control. 6-11 HR controls. B) Results of the HR test. PTI strength was scored on a 0-3 scale. Significant difference from maximum PTI (no HR, pre-inoculation nr. 5) calculated by student's *t*-test is marked by a * ($p < 0.05$). C) Representative leaves with typical HR patterns. Numbers correspond to pre-inoculations in table A. HR spots appearing because of reduced PTI are marked with a red arrow. Abbreviations: 1. C4H inhibitor: Piperonylic acid (PIP), 2. PAL inhibitor: Aminoxyacetic acid (AOAA), 3. 4CL inhibitor, 3,4-Methylenedioxy cinnamic acid (MDCA), 4. F5H inhibitor: Coniferyl aldehyde (ConAld), hrcC: *P. syringae* pv. *syringae* hrcC-.

The degree of HR was noted 2 days later. When inhibitors and PTI inducing bacteria were combined, a significant reduction in PTI occurred in the case of C4H inhibition as expected, and even more pronouncedly, PAL inhibition. Normal PTI developed in the case of F5H inhibition and 4CL inhibition. When the inhibitors were injected alone, full HR was observed after the challenging infections, while no symptoms occurred when challenging inoculation was omitted, so the inhibitors alone did not affect HR induction.

Identification of phenolic compounds putatively related to PTI from tobacco leaves

We have used high-performance liquid chromatography-diode array detection-mass spectrometry (HPLC-DAD-MS) to find PTI-related phenolic compounds. Development of the extraction method from *Nicotiana* leaves included testing different solvents, extraction times and temperatures, based on recommendations in literature (Cho et al. 2012). To monitor extraction efficiency, samples were divided, and a standard mixture (cinnamic acid, p-coumaric acid, caffeic acid, salicylic acid, quercetin, rutin, scopoletin) was spiked into half of each sample before extraction. Extraction efficiency in our hands was best when using 90% aqueous methanol, and heating the samples (70 °C).

Later we further improved the sample preparation method, the extracts of plant phenolics were purified by SPE (solid phase extraction) and were concentrated prior to HPLC analysis. We also added an internal standard – *o*-anisic acid – not present in tobacco extracts. This was suitable as a normalization factor to correct for phenolics losses occurring during extraction. This improved method enabled the detection of further phenolic compounds present during PTI.

N. benthamiana leaves were infiltrated with *Pseudomonas syringae* pv. *syringae* hrcC-suspension or Flg22 peptide to induce PTI, and water as a control. Leaf samples were taken 6 hours later and extracts were analysed by HPLC-DAD-MS. Several, initially unknown phenolic compounds (with characteristic UV spectrum) were found to be more abundant in PTI-induced *N. benthamiana* leaves than in water treated controls (Table 1, compound names are already indicated, methods of identification are described in the following sections). Both PTI inducers were used at concentrations that caused reliable HR-inhibition at 6 h.p.i. (Flg22 at 50 µM, *P. syringae* hrcC- at 10⁹ CFU/ml). At these concentrations, Flg22 peptide triggered higher accumulation of most analysed phenolics.

Compound name	Rt (min)	m/z [M-H]- or [M+H]+	Relative accumulation	
			HRCC/W	FLG22/W
N-caffeoyl-putrescine isomer 1	1.53	249(-)	1.60	2.91
N-caffeoyl-putrescine isomer 2	1.82	249(-)	1.01	3.19*
Neochlorogenic acid	2.77	353(-)	1.43*	1.77**
Unknown	2.90	205(+)	1.27	3.07*
Chlorogenic acid	3.87	353(-)	1.14	2.57**
Cryptochlorogenic acid	4.24	353(-)	1.21	2.58**
Chlorogenic acid isomer1	4.53	353(-)	1.20	2.86*
Chlorogenic acid isomer 2	5.74	353(-)	1.06	2.29**
Unknown	6.10	303(+)	1.26	3.88*
Unknown	7.90	181(+)	1.34	4.28*
Acetosyringone	10.00	197(+)	12.52*	18.32*
Unknown	10.40	291(+)	1.59	3.79*
Unknown	10.80	197(+)	1.52	3.94*

Table 1. Major PTI-induced phenolic compounds in water treated control (W) and PTI induced *N. benthamiana* leaves. Retention times (Rt) correspond to the separation by HPLC-DAD-MS. Mass-to-charge ratio (m/z) value of the molecular ion was determined by MS using electrospray ionization (ESI) in the negative mode. Relative accumulation values correspond to the ratio of the mean content of each compound in the PTI-induced (*Pseudomonas syringae* pv. *syringae* hrcC- and Flg22 treated) versus the mean value obtained for the water treated control, 6 h.p.i. At least three plants were analysed for each treatment. Significant difference from water treated control is marked by a * (*

$p < 0.1$, $** p < .05$). Tentative identification of the compound names indicated in the table was carried out later, after MS/MS and HRMS analysis.

To identify the putatively PTI-related compounds, high-performance liquid chromatography – tandem mass spectrometry (HPLC-MS/MS) analysis of phenylpropanoid compounds from PTI-induced and water injected control *N. benthamiana* leaf samples was performed at the Faculty of Pharmacy, Semmelweis University.

Three compounds yielded the same mass signal assigned to be their deprotonated molecule at m/z 353 $[M-H]^-$. Based on the MS/MS fragmentation spectra the compounds were tentatively identified as 3-caffeoyl quinic acid (chlorogenic acid), 4-caffeoyl quinic acid (cryptochlorogenic acid) and 5-caffeoyl quinic acid (neochlorogenic acid). The identity of these compounds was confirmed by HPLC-MS using analytical standards in our laboratory.

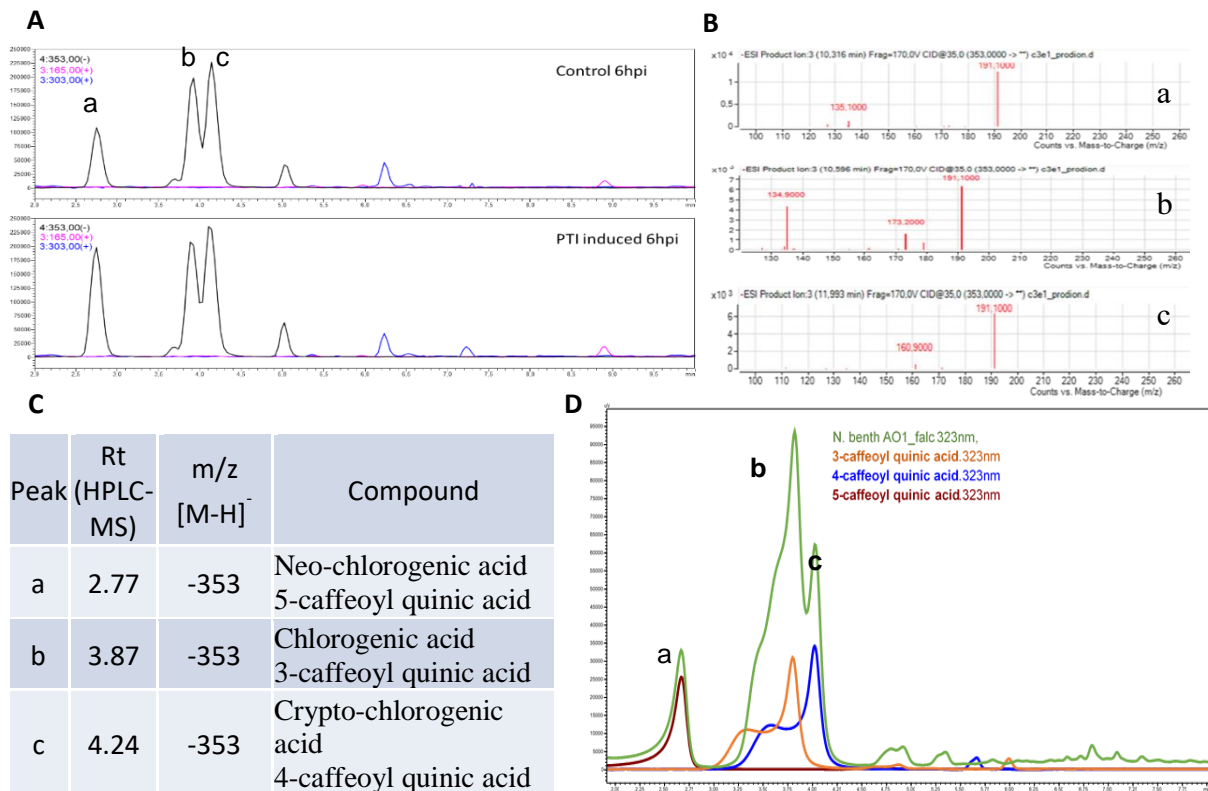


Fig. 13. Identification of PTI-related phenolic molecules as isoforms of chlorogenic acid by HPLC-MS/MS. A) HPLC-MS analysis of phenolic compounds from PTI-induced and water treated control *N. benthamiana* leaves. Selective ion monitoring chromatogram. PTI was induced by *Pseudomonas syringae* pv. *syringae* hrcC- bacteria. Samples were taken 6 hpi. B) MS/MS fragmentation spectra of the m/z 353 ions of compounds corresponding to peaks a, b and c. C-D) Identity of compounds a, b and c was confirmed using analytical standards. HPLC-DAD chromatograms at 323nm.

We identified a further compound (m/z 197 $[M+H]^+$) selectively occurring in PTI-induced (6 hpi) leaves as acetosyringone (3,5-dimethoxy-4-hydroxyacetophenon), by comparison of its MS and UV spectra and retention time to those of an analytical standard (Fig. 14.). Besides *P. syringae* hrcC- treatment, acetosyringone was also strongly induced in flg22 peptide treated leaves, but was not detectable in water treated controls, as indicated in Table 1.

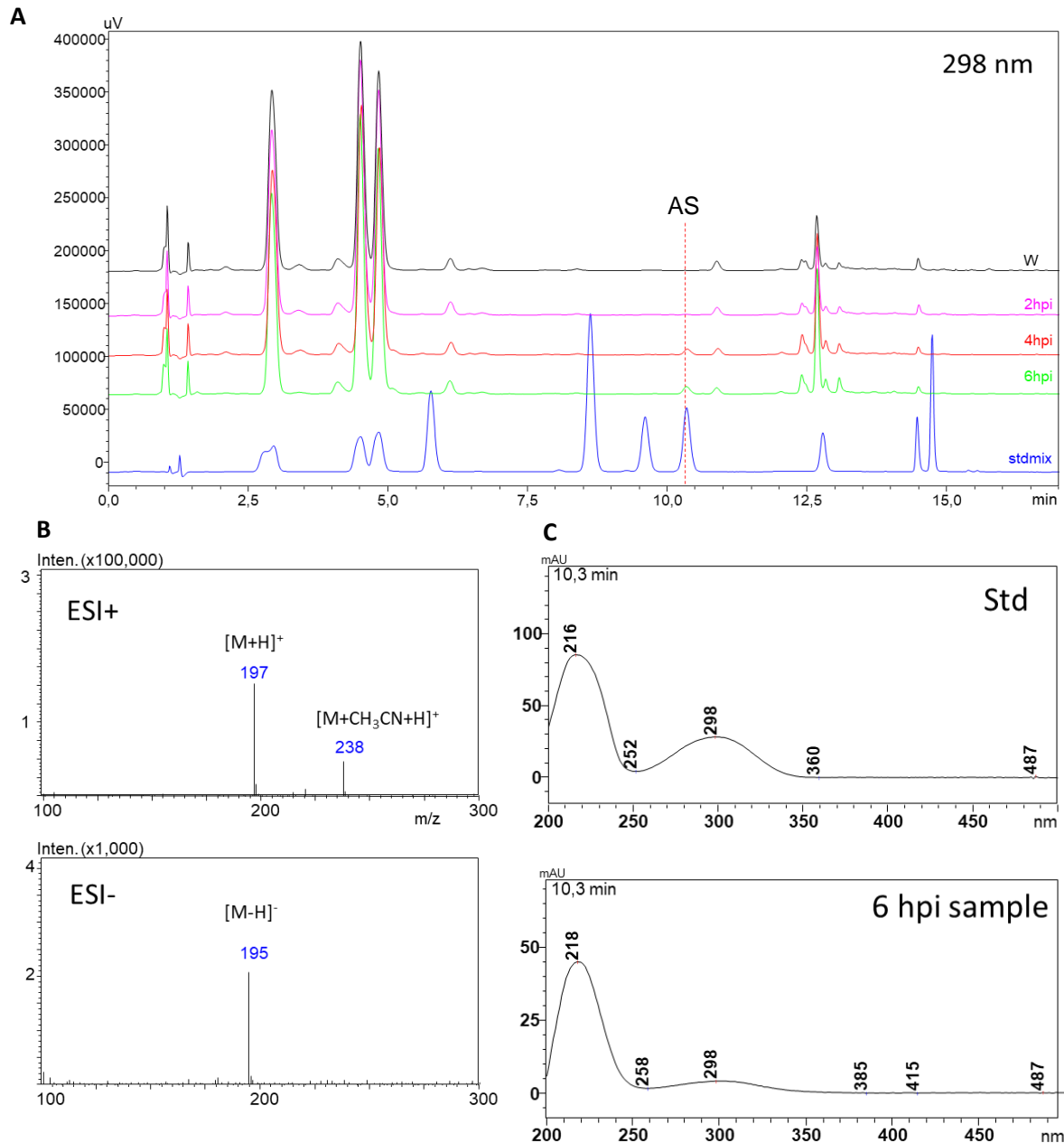


Fig. 14. Identification of a PTI-related phenolic compound as acetosyringone (AS) by HPLC-DAD-MS using analytical standard. A) HPLC-DAD analysis of phenolic compounds from PTI-induced and water treated control *N. benthamiana* leaves detected at 298 nm. PTI was induced by *Pseudomonas syringae* pv. *syringae* hrcC- bacteria, water was injected as control. Samples were taken 2, 4, 6 hpi. B) MS spectra of acetosyringone in both positive and negative modes. It had the expected m/z values in both positive and negative modes. C) Identity of acetosyringone was supported by the similar UV spectra of the analytical standard and the unknown peak. Abbreviations: AS: acetosyringone, Std: standard.

A further phenolic compound (m/z 249 [M-H]⁻), which accumulated differentially between control and PTI-induced leaves was identified as N-caffeoyl-putrescine at the Metabolomics Platform of the Plant Physiology Department, Agricultural Institute, CAR HAS. This was identified based on LC-HRMS/MS fragmentation spectra in +/- modes. The main fragments corresponded to the fragmentation patterns available in literature (Shakya and Navarre 2006). Moreover, the measured accurate mass: 249.1223 (-) of the compound supported its identification as N-caffeoyl-putrescine as well (Fig. 15).

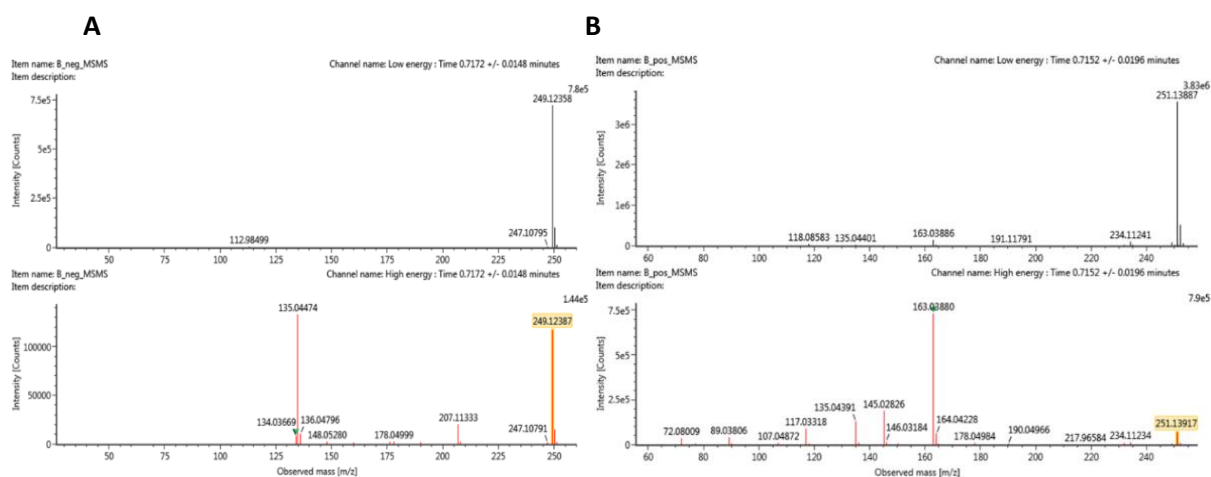


Fig. 15. LC-MS/MS fragmentation spectra of the compound *N*-caffeoyl-putrescine in ESI negative (A) and positive (B) modes using lower (above) and higher (below) fragmentation energies.

High throughput HRMS and MS/MS measurements became available only in the extension period of the project, as a metabolomics platform was newly established at the Agricultural Institute of our research centre. Higher scale identification of compounds present in PTI-induced and control *N. benthamiana* samples was possible at this stage (qualitative study). High scale quantitative analysis would be available in the future at the novel facility. A study on the metabolomics of Flg22 treated (i.e. PTI-induced) *N. tabacum* cell suspensions was published by Mhlongo et al. in 2016. As a first step in deciphering higher throughput metabolomics of PTI we assessed the detectability of the Flg22-induced or -repressed compounds reported in the above publication (Table 2).

Most of the compounds reported to be more abundant in Flg22 treated tobacco cell culture were detected in our leaf samples. Identifications were based on high resolution accurate mass values, and MS/MS ion fragmentation spectra in both positive and negative ion modes, where it was possible. Representative fragments were compared to published fragment patterns. Identification of the metabolites was carried out at the Metabolomics Platform of the Plant Physiology Department, Agricultural Institute, CAR HAS. As high throughput metabolomics studies of PTI are scarce, it would be worth to carry out more extensive studies in the future.

Molecular formula	Mass provided*	Accurate mass measured	Compound name	Flg22 Regulated*	Detected WATER treated	Detected Flg22 treated
C16H16O7	319.078	319.0823	p-Coumaroylshikimic acid	U	•	
C16H16O8	335.051	335.0772	3-Caffeoylshikimic acid		••	••
	335.071		4-Caffeoylshikimic acid	U	••	••
	337.085		Unknown	U	••	•
C16H18O8	337.194	337.0929	5-p-Coumaroylquinic acid	U	•••	••
	348.176		Unknown			
	353.077		cis-5-Caffeoylquinic acid	U	•••	•••
	353.085		trans-5-Caffeoylquinic acid	U	•••	•••
	353.086		3-Caffeoylquinic acid	U	•••	•••
	353.086		cis-4-Caffeoylquinic acid		•••	•••
	353.101		trans-4-Caffeoylquinic acid	D	•••	•••
C16H20O9	355.091	355.1035	Feruloylglycoside			
	355.092	355.1035	Feruloylglycoside			
	355.099	355.1035	Feruloylglycoside			
C17H20O9	367.104	367.1035	5-Feruloylquinic acid	U	••	••
C19H28N2	411.172		Caffeoylputrescine glycoside	U		
	443.15		Unknown			
C23H27NC	444.145		Coumaroyltyramine glycoside isomer			
	444.161		Coumaroyltyramine glycoside isomer			
C24H29NC	474.172	474.177	Feruloyltyramine glycoside isomer	U	••	••
	474.175		Feruloyltyramine glycoside isomer	U	••	••
	474.181		Feruloyltyramine glycoside isomer	U	••	••
	474.184		Feruloyltyramine glycoside isomer	U	••	••
	499.188		Unknown		••	••
C25H31NC	504.182	504.1875	Feruloyl-3-methoxytyramine glycoside	D	•	•
	515.12		4,5-diCaffeoylquinic acid	U	•	•
C22H28O1	515.141	515.1406	3-O-(4'-O-Caffeoylglucosyl) quinic acid		•	
	515.142		5-O-(3'-O-Caffeoylglucosyl) quinic acid		•	
C25H24O1	515.161	515.1195	3,4-diCaffeoylquinic acid	U	•	•
	546.194		Feruloyl-3-methoxytyramine conjugate isomer	D		
	546.196		Feruloyl-3-methoxytyramine conjugate isomer	U		
	587.236		Unknown			

Table 2. UHPLC-MS diagnostic ions (ESI-negative mode) used for the identification of biomarkers in Flg22 MAMP elicited tobacco cells (data from Mhlongo et al. 2014 are denoted with *) compared to leaf samples (own data, grey shading). Metabolites positively and negatively correlated with Flg22 treatment in the publication of Mhlongo et al. are indicated with U and D respectively. Metabolites detected in water treated control or Flg22 treated leaf samples are denoted with •, •• or ••• depending on relative abundance (measurements were not quantitative).

Using HPLC-DAD-MS and HRMS/MS we detected some PTI-related compounds in tobacco leaves that were not reported by Mhlongo et al. from tobacco cell cultures. We were able to annotate two of these metabolites as acetosyringone and N-caffeoyl-putrescine. During PTI and other resistance mechanisms, processes in the extracellular space are known to play an important role (Ott et al. 2012). Acetosyringone itself was first isolated from *N. tabacum* leaf exudates and root culture medium, where it was established to be exudate specific, not passively leaking out from damaged plant cells (Stachel et al. 1985). So in the case of plant cell cultures, it would be worth analysing the cell culture media for interesting metabolites as well.

Changes in phenolic metabolite levels

To see differences between metabolite patterns corresponding to different plant-bacterium interactions, we analysed samples from *N. benthamiana* leaves injected with suspensions of a compatible bacterium: *Pseudomonas syringae* pv. *tabaci* (PTAB), two incompatible bacteria: *P. syringae* DC3000 and *P. syringae* 61 (PS61), PTI inducing bacterium: *P. syringae* hrcC-, and a PTI inducing MAMP: flg22 peptide. One half of each leaf was injected with a suspension, and the other half with water; samples were taken at 6 hpi. The three chlorogenic acid isoforms were more abundant in the PS61, flg22 and DC3000 and PTAB treated samples than in water controls. This was more pronounced in the flg22 and PS61 samples. In the *P. syringae* hrcC- and *P. tabaci* samples the difference was moderate. Chlorogenic acids seem to be present at elevated levels independently of the type of plant-bacterium interaction. On the contrary, acetosyringone displayed a more unique pattern: it was only detectable in flg22 and *P. syringae* hrcC- treated samples – the two PTI induced samples, but it was absent (below detection limit) in the rest of the samples at the used concentrations, at 6 h.p.i.

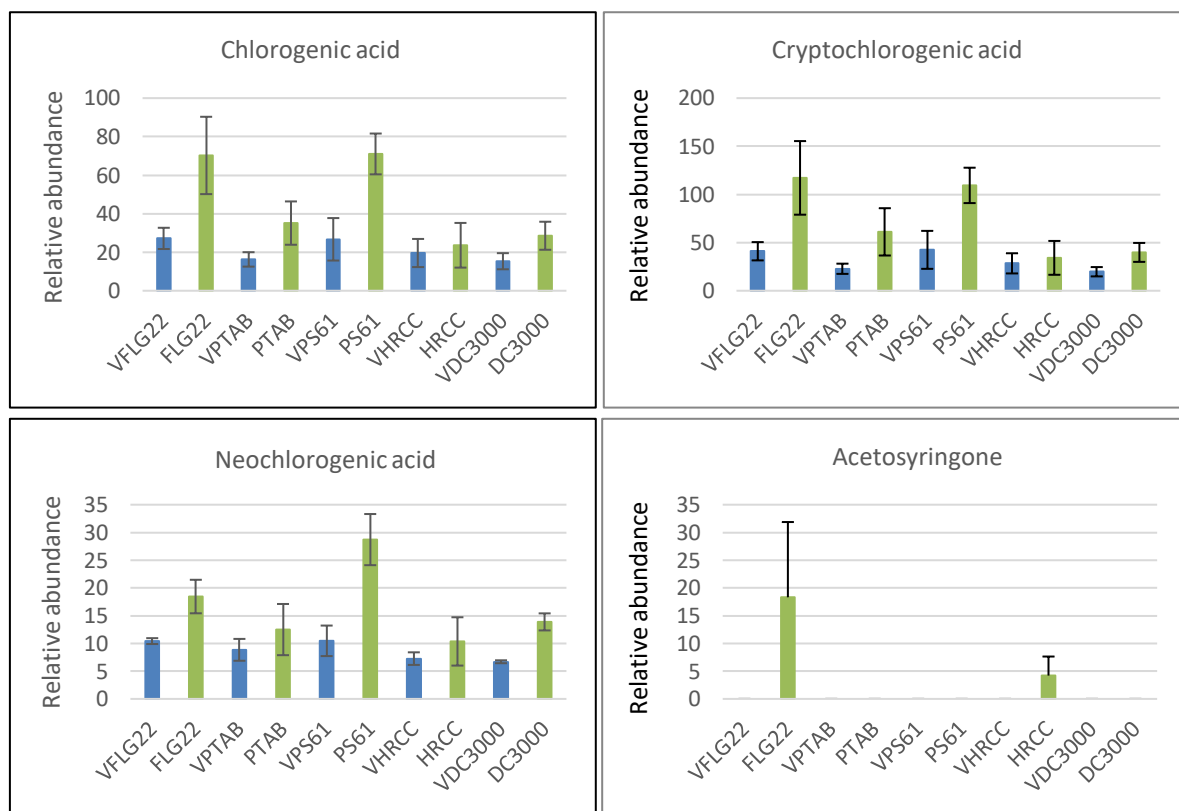


Fig. 16. Relative accumulation of different phenolics in *N. benthamiana* leaves in response to treatments with different bacteria 6 h.p.i. Water control was included on each bacterial treated leaf. All values were normalized with non-treated leaf control levels. Error bars indicate SEM n=3. V: water control; P61: *P. syringae* pv. *syringae* 61; HRCC: *P. syringae* hrcC mutant; TAB: *P. syringae* pv. *tabaci*.

Time course experiment supported the gradual accumulation of acetosyringone during the course of the build-up of effective PTI. It is worth noting that inhibition of HR and of proliferation of compatible bacteria upon challenge inoculation is usually effective 5-6 hours after induction of PTI.

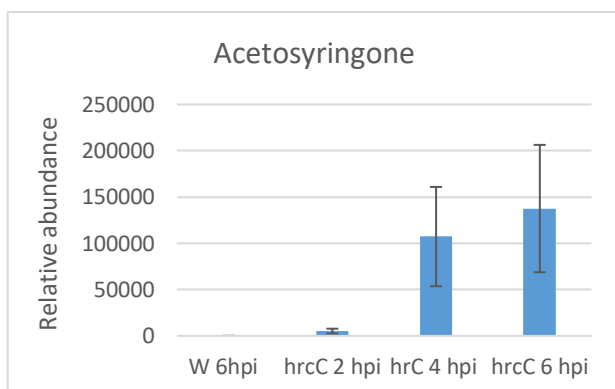


Fig. 17. Relative accumulation of acetosyringone in *N. benthamiana* leaves in response to treatments with *P. syringae* pv. *syringae* hrcC- bacteria 2, 4 and 6 h.p.i. All values were normalized with non-treated control levels. Error bars indicate SEM n=3. W: water treated control; hrcC: *P. syringae* hrcC mutant.

Metabolite patterns in the VIGS plants were also analysed to see if silencing of phenylpropanoid genes caused any measurable differences. It was most remarkable that in the dwarfed 4CL silenced leaves two new (unidentified) peaks could be detected, absent from all other samples. Acetosyringone was not detectable in PTI induced 4CL silenced leaves, while it was present in all other PTI induced VIGS plants (Fig. 18.).

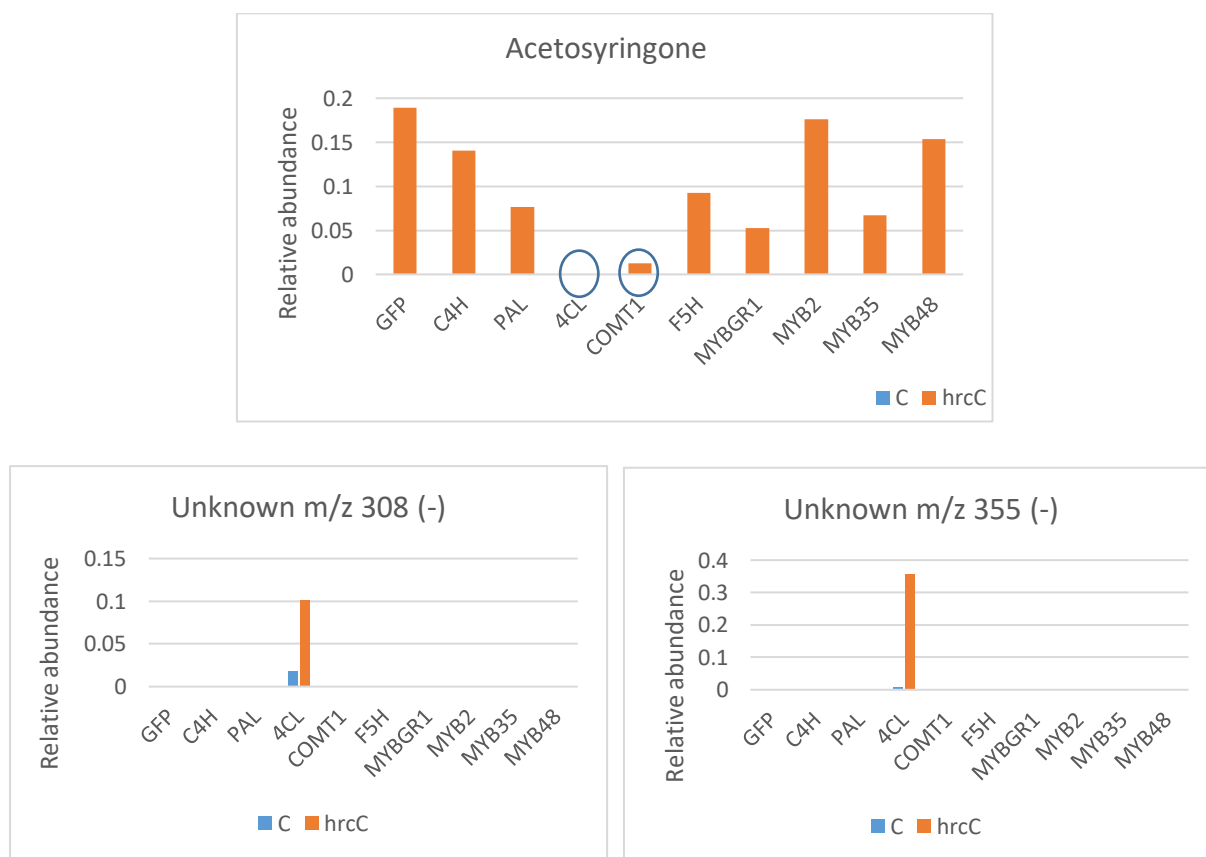


Fig. 18. Differential accumulation of metabolites in *N. benthamiana* leaves silenced in certain phenylpropanoide and MYB genes in response to treatments with *P. syringae* pv. *syringae* hrcC- bacteria, 6 h.p.i W: water treated control; hrcC: *P. syringae* hrcC mutant.

Effects of phenolic compounds on bacteria

Direct effects

PTI-specific changes of cinnamic acid and coumaric acid have been detected earlier in our laboratory (Szatmári et al. 2014), so we tested the effect of these substances and caffeic acid on in planta proliferation and in vitro viability of compatible pathogenic *P. syringae* pv. *tabaci*. Bacteria were combined with 10 or 100 micromolar concentrations of the studied substances. 4-hour co-incubation with *P. tabaci* had no effect on viability of bacteria at 10 micromolar concentrations. At 100 micromolar concentrations caffeic acid caused 1000x drop in bacterial CFU, while coumaric acid and cinnamic acid caused cca. 100x reduction.

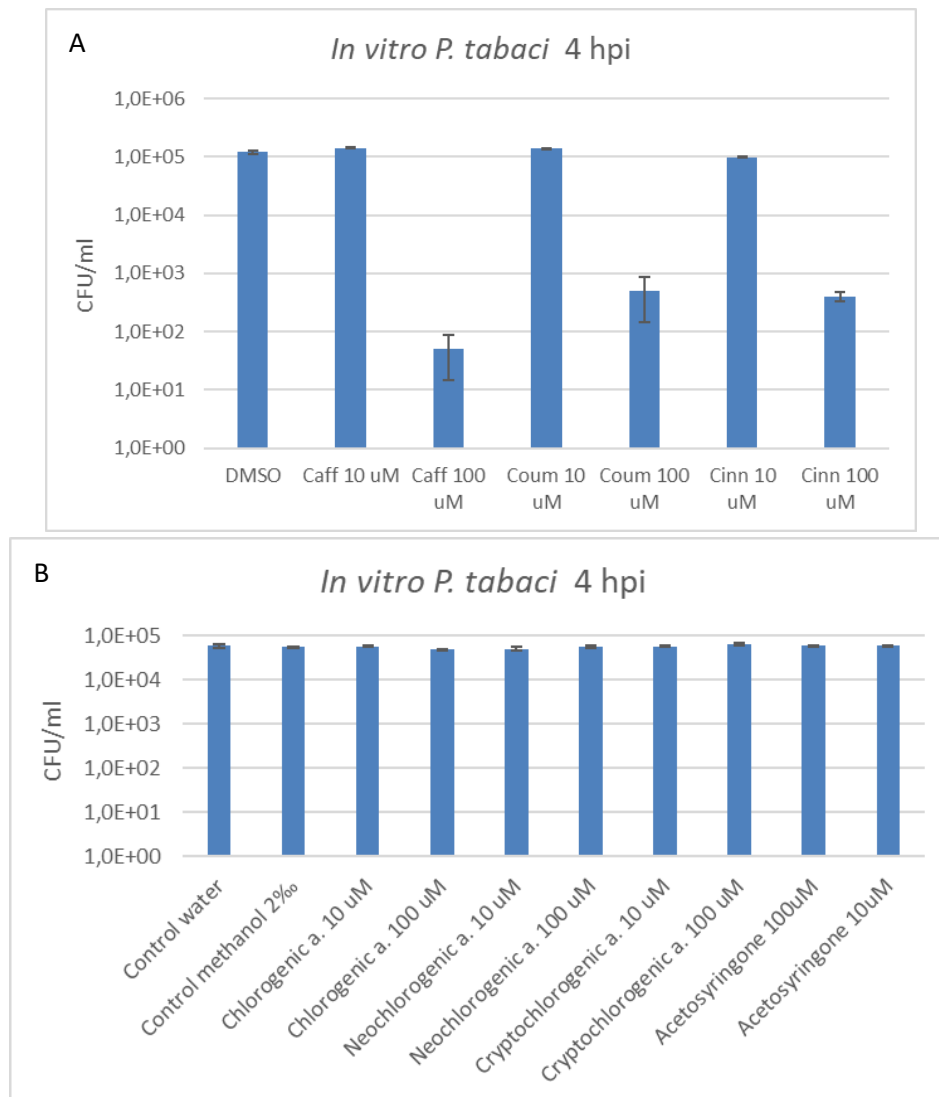


Fig. 19. Fig. 3. In vitro effect of phenolic metabolites on the growth of *P. tabaci* at 10 and 100 micromolar concentrations. A) Caffeic acid (Caff), Coumaric acid (Coum), Cinnamic acid (Cinn). B) Chlorogenic acid, Neochlorogenic acid, Cryptochlorogenic acid and Acetosyringone.

We also examined the effect of chlorogenic acid, neochlorogenic acid, cryptochlorogenic acid and acetosyringone in vitro on the viability of compatible pathogenic *P. syringae* pv. *tabaci*. Bacteria were combined with 10 or 100 micromolar concentrations of the studied compounds. 4-hour co-incubation had no effect on the viability of bacteria at 10 nor at 100

micromolar concentrations. In contrast to the other tested compounds (coumaric acid, caffeic acid and cinnamic acid) - chlorogenic acid, neochlorogenic acid, cryptochlorogenic acid and acetosyringone do not seem to have direct antibacterial activity on *P. tabaci* at the tested concentrations, although higher concentrations could be effective. For example Kröner et al. (2011) found that chlorogenic acid accumulation directly correlated to PAL induction in potato, causing active defence against *Pectobacterium atrosepticum* in tubers. In vitro it was effective when added to the culture medium at a concentration of 1 mmol/L (10 times the largest concentration used by us). At a lower concentration of 0.6 mmol/L, growth inhibition was not significant.

Indirect effect of acetosyringone

Several sources reported that acetosyringone or related acetophenones have antifungal or antibacterial effects. Lorimer and Perry (1993) reported isolation of two major antifungal active components from *Plagiochila fasciculata* (New Zealand liverwort). These were identified as 2-hydroxy-4,6-dimethoxyacetophenone and 2-hydroxy-3,4,6-trimethoxyacetophenone. The relatively high activity of the crude extract was due to the high level of these compounds in the plant (6-7 mg/g dried plant for both). In vitro oxidation of acetosyringone with hydrogen peroxide by a peroxidase can create a prolonged oxidative environment similar the oxidative burst in tobacco suspension cells inoculated with incompatible bacteria according to Mock et al. (2015).

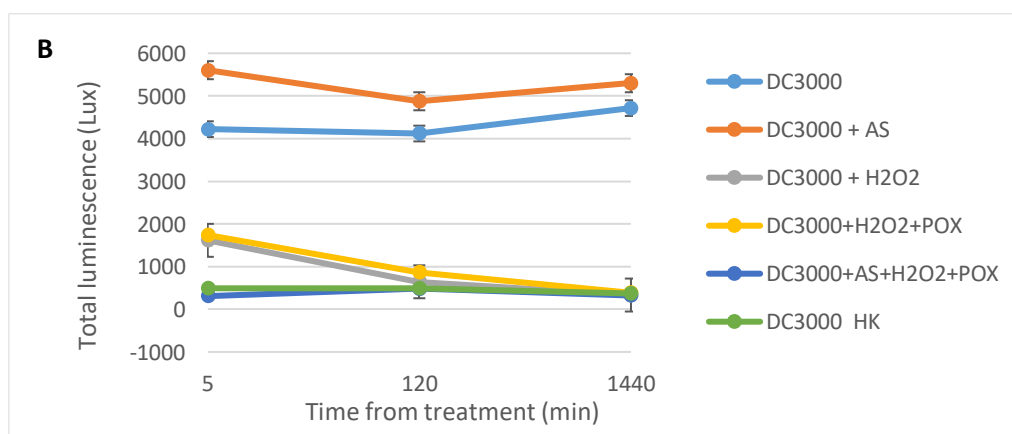
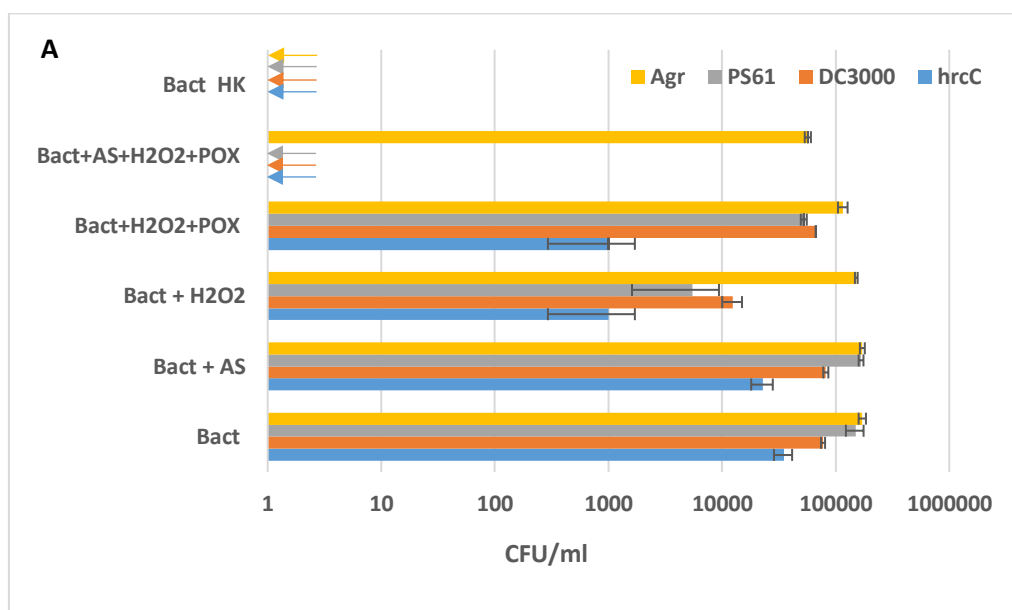


Fig. 20. Indirect antimicrobial effect of acetosyringone on plant pathogenic bacteria. **A)** Antimicrobial effect of oxidized acetosyringone on different plant pathogenic bacteria. 10^5 CFU/ml bacteria were added to reaction mixtures containing 50 mM acetosyringone, 50 mM H_2O_2 , and 0.72 U/ml horseradish peroxidase, and various control mixtures from which one or two components were omitted. Serial dilutions were plated following 3 hours of co-incubation, for CFU determination. **B)** A similar assay was conducted with *P. syringae* DC3000 lux, a luminescent *P. syringae* strain and bioluminescence was measured at certain time points. AS: acetosyringone, HK: heat killed, Agr: *Agrobacterium tumefaciens*, PS61: *Pseudomonas syringae* pv. *syringae* 61, hrcC: *Pseudomonas syringae* pv. *syringae* hrcC-, DC3000: *Pseudomonas syringae* pv. *tomato* DC3000, DC3000Lux: luminescent DC3000 strain, POX: horse radish peroxidase.

We tested if in vitro oxidation of acetosyringone results in antimicrobial effects against bacterial strains corresponding to different plant (tobacco)-bacterium interactions (Fig. 20. A.). Two incompatible bacteria: *P. syringae* pv. *tomato* DC3000 and *P. syringae* pv. *syringae* 61 (PS61), and the PTI inducing bacterium *P. syringae* hrcC- (hrcC). *Agrobacterium tumefaciens* was also tested, as its virulence genes are activated by acetosyringone, and it is known to be able to evade PTI. We combined 50 μ M acetosyringone, 50 μ M H_2O_2 and 0.72 U/ml peroxidase in phosphate buffer, containing 10^5 CFU/ml suspensions of different bacteria. Serial dilutions were plated after 3 hours of co-incubation. No growth of the *Pseudomonas* strains was detected after incubation in the complete reaction mixture. On the contrary, *Agrobacterium* growth was not impaired at all. When omitting different components of the mixture, *Pseudomonas* were still inhibited to various extent. In our hands, *P. syringae* hrcC- seemed to be more susceptible than the other two strains. Acetosyringone alone was not effective against any of the four strains, so the combination of acetosyringone with peroxidase activity is essential. Activation of peroxidase activity at the time interval of acetosyringone production during PTI has been shown earlier (Bozsó et al. 2005). Wu and Pan (2000) have shown that an *Agrobacterium* strain deficient in catalase activity was highly attenuated in the ability to cause tumours on plants compared with the wild type. Thus catalase was considered a virulence factor of *Agrobacterium*, and our results might provide a possible explanation for an antioxidant enzyme being a virulence factor.

We used a chromosomally luxCDABE-tagged *P. syringae* strain, luminescent *P. syringae* DC3000 lux (Fan et al. 2008) to monitor the changes in bacterial cell viability caused by oxidized acetosyringone. Viable *P. syringae* DC3000 lux actively emit a constant level of luminescence. We planned to monitor the time dependent lowering of luminescence of bacteria when combined with oxidized acetosyringone. We found that luminescence level was dropped to background level already at the first measurement (5 minutes) after administration of the acetosyringone+ H_2O_2 +peroxidase cocktail (Fig. 20. B.) This response was significantly faster than the effect caused by H_2O_2 alone or H_2O_2 combined with peroxidase. Acetosyringone alone did not have any effect on bioluminescence.

These results together indicated that acetosyringone, a tobacco metabolite specifically appearing after PTI induction either by *P. syringae* HR- bacteria or Flg22 elicitor at the time point (6 h.p.i.) when PTI starts to be effective against bacterial multiplication, causes a rapid inactivation of certain plant pathogenic bacteria, when in an oxidative environment. We reported induction of peroxidase genes and peroxidase activity during PTI earlier, so the presence of acetosyringone might indeed have an important role in the inhibition of bacterial proliferation during PTI.

Measurement of hrp gene activity changes of *Pseudomonas syringae* pv. *tabaci* in response to various phenolic molecules by real-time RT-PCR

Plant pathogenic *Pseudomonas* bacteria use the Type III secretion system (T3SS) to inject effector proteins into host cells. Assembly of the T3SS is dependent on the hrp genes and is necessary for virulence. We measured in planta transcriptional activation of three hrp genes (hrp K, L, R) of *Pseudomonas syringae* pv. *tabaci* in response to various phenolic acids to see, if they are able to interfere with hrp gene activity, possibly acting as putative signal molecules.

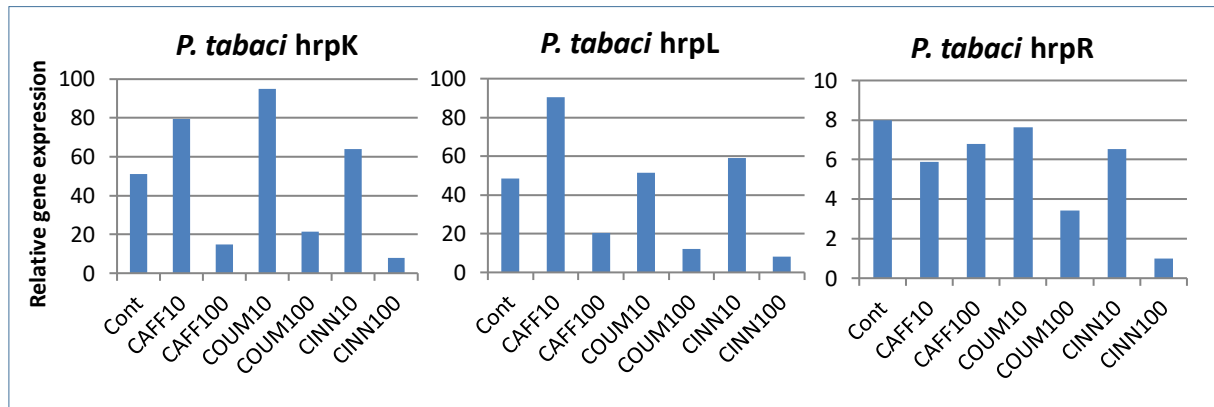


Fig. 21. Expression of type III secretion system (T3SS) genes in the *P. tabaci* treated with different phenolic acids. Relative expression of the hrpK, hrpL and hrpR genes was measured by quantitative real-time reverse transcription-polymerase chain reaction (RT-PCR). The bacterial 16S rRNA gene was used as a constitutive control.

10 and 100 micromolar quantities of caffeic, coumaric and cinnamic acids were co-infiltrated into *N. tabacum* leaves together with *P. tabaci* and RNA was isolated 4 hours later. Transcriptional activity of bacterial hrp genes was evaluated by real time RT-PCR, each value was normalized by measured constitutive 16S rRNA levels.

Previous experiments regarding the antimicrobial effects of caffeate, coumarate and cinnamate on *Pseudomonas syringae* pv. *tabaci* implied that each caused 100-1000x drop in bacterial CFU counts at 100 micromolar concentration, while they had no effect at 10 micromolar concentrations in vitro. Transcriptional activities of all measured hrp genes (K, L, R) were significantly lower in bacteria treated with 100 micromolar solutions of phenolic acids than in controls (3-10 fold reduction, normalized with constitutive 16S rRNA levels). These results suggest possible role of the investigated phenolic acids in repression of certain hrp genes of *Pseudomonas syringae* pv. *tabaci* at a higher (100 micromolar) concentration.

Conclusions

Cinnamic acid-4-hydroxylase seems to catalyse an important reaction necessary for effective PTI, as gene silencing in *N. benthamiana* and *Arabidopsis*, overexpression and pharmacological inhibition each significantly altered PTI efficiency. The other investigated phenylpropanoid (*PAL*, *COMT*, *F5H*) enzymes might also play an important role, because certain ways of inhibition or overexpression caused altered PTI. Enzymatic reactions catalysed by them might however be redundantly conducted by several isoenzymes, therefore complete inhibition is hard to reach.

Silencing of two MYB genes – NtMYBGR1 and NtMYB2 - known from literature to alter phenylpropanoid gene expression decreased PTI efficiency. Only one of them (NtMYBGR1) was successfully cloned for overexpression, but this did not result in enhanced resistance. This

discrepancy could be investigated in the future, as the mechanism by which MYB factors control gene activation is still unclear. Post translational modifications such as poly-ADP-ribosylation and phosphorylation seem to alter their activity (Zhao and Dixon 2011). However, the biological importance of such modifications in planta is currently unknown yet.

Several metabolites were detected and some identified during PTI activation, by HPLC. Three isoforms of chlorogenic acid accumulated in response to different treatments with bacteria and the MAMP flg22 peptide. This accumulation was not specific for PTI, as it occurred in the case of compatible and incompatible pathogens as well. Acetosyringone was only detected in the PTI-induced (flg22 and *P. syringae hrcC*-) samples at 6 hpi. This was especially interesting, as it was found to rapidly inhibit several phytopathogenic *Pseudomonas* bacterium species, when combined with hydrogen peroxide and horse radish peroxidase. These results are even more interesting as over-expression of cinnamate 4-hydroxylase has been shown to increase the accumulation of acetosyringone in elicited tobacco cell-suspension cultures (Blount et al. 2001). Moreover, an O-methyltransferase synthesising acetosyringone was found in methyl jasmonate-treated tobacco cell-suspensions cultures (Negrel et al. 2014). These changes in acetosyringone levels in our C4H and OMT overexpressing constructs will be analysed in the future.

During this OTKA/NKFIH project we managed to reveal some important elements of the mechanisms possibly leading to inhibition of bacteria during pattern triggered immunity. Apart from some phenolic acids directly inhibiting bacterial growth, it seems that the interplay of a phenolic compound (acetosyringone) and the oxidative burst (generated by hydrogen peroxide and peroxidase) might enhance antibacterial activity.

Results of the project have partly been published in international journals and international and Hungarian conferences. Some important results will be published in the future, in manuscripts being prepared on the effects of downregulation of phenylpropanoid enzymes on pattern triggered immunity; and on the changes in phenolic metabolite levels during PTI, and the antimicrobial effects of some of these compounds.

Citations

Asselin JAE, Lin J, Perez-Quintero AL, Gentzel I, Majerczak D, Opiyo SO, Zhao W, Paek SM, Kim MG, Coplin DL., Blakeslee JJ., Mackey D (2015) Perturbation of maize phenylpropanoid metabolism by an AvrE family type III effector from *Pantoea stewartii*. *Plant Physiology* 167 (3) 1117-1135; DOI: 10.1104/pp.114.253120

Blount JW, Masoud S, Sumner LW, Huhman D, Dixon RA (2002) Over-expression of cinnamate 4-hydroxylase leads to increased accumulation of acetosyringone in elicited tobacco cell-suspension cultures. *Planta* 214: 902-910 DOI 10.1007/s00425-001-0701-5

Bozsó Z, Ott PG, Kaman-Toth E, Bognar GF, Pogany M, Szatmári, Á. (2016) Overlapping yet response-specific transcriptome alterations characterize the nature of tobacco-*Pseudomonas syringae* interactions. *Front. Plant Sci.* 7:251. doi: 10.3389/fpls.2016.00251

Bozsó Z, Ott PG, Szatmari A, Czalleng A, Varga G, Besenyi E, Sárdi É, Bányai É, Klement Z (2005) Early detection of bacterium-induced basal resistance in tobacco leaves with diaminobenzidine and dichlorofluorescein diacetate. *Journal of Phytopathology*, 153: 596-607. doi:10.1111/j.1439-0434.2005.01026.x

Chezem WR, Memon A, Li F-S, Weng J-K, Clay NK (2017) SG2-Type R2R3-MYB Transcription Factor MYB15 Controls Defense-Induced Lignification and Basal Immunity in *Arabidopsis* *The Plant Cell*, Vol. 29: 1907–1926

- Chisholm ST, Coaker G, Day B, Staskawicz BJ (2006) Host-microbe interactions: shaping the evolution of the plant immune response. *Cell* 124, 803–814
- Cho K, Kim Y, Wi SJ, Seo JB, Kwon J, Chung JH, Park KY, Nam MH (2012) Nontargeted metabolite profiling in compatible pathogen-inoculated tobacco (*Nicotiana tabacum* L. cv. Wisconsin 38) using UPLC-Q-TOF/MS. *J Agric Food Chem* 60(44):11015–11028
- Daudi A, Cheng Z, O'Brien JA, Mammarella N, Khan S, Ausubel FM, Bolwell GP (2012) The apoplastic oxidative burst peroxidase in *Arabidopsis* is a major component of pattern-triggered immunity. *The Plant Cell* 24 (1) 275-287; DOI: 10.1105/tpc.111.093039
- Fan J, Crooks C, Lamb C. (2008) High-throughput quantitative luminescence assay of the growth in planta of *Pseudomonas syringae* chromosomally tagged with *Photobacterium luminescens luxCDABE*. *Plant J.* 53:393–399
- Fodor J, Kámán-Tóth E, Dankó T, Schwarczinger I, Bozsó Z, Pogány M (2018): Description of the *Nicotiana benthamiana*–*Cercospora nicotianae* Pathosystem, *PHYTOPATHOLOGY* 108:1 149-155
- Fraser CM and Chapple C (2011) The phenylpropanoid pathway in *Arabidopsis*. *The Arabidopsis Book*. doi/10.1199/tab.0152
- Frerigmann H, Piślewska-Bednarek M, Sánchez-Vallet A, Molina A, Glawischnig E, Gigolashvili T, Bednarek P (2016). Regulation of pathogen-triggered tryptophan metabolism in *Arabidopsis thaliana* by MYB transcription factors and indole glucosinolate conversion products. *Mol. Plant* 9: 682–695.
- Gaquerel E, Gulati J, Baldwin IT. (2014) Revealing insect herbivory-induced phenolamide metabolism: From single genes to metabolic network plasticity analysis. *Plant J.* 2014;79:679–92.
- Huang J, Gu M, Lai Z, Fan B, Shi K, Zhou YH, Yu JQ, Chen Z. (2010) Functional analysis of the *Arabidopsis* PAL gene family in plant growth, development, and response to environmental stress. *Plant Physiol.* 153(4):1526-38. doi: 10.1104/pp.110.157370.
- Kachroo A, Vincelli P, Kachroo P (2017) Signaling mechanisms underlying resistance responses: what have we learned, and how is it being applied? *Phytopathology*,. doi:10.1094
- Kámán-Tóth E, Pogány M, Dankó T, Szatmári Á, Bozsó Z. (2018) A simplified and efficient *Agrobacterium tumefaciens* electroporation method. *3 Biotech.* 8(3):148. doi:10.1007/s13205-018-1171-9
- Kishi-Kaboshi M, Seo S, Takahashi A, Hirochika H (2018) The MAMP-Responsive MYB transcription factors MYB30, MYB55 and MYB110 activate the HCAA synthesis pathway and enhance immunity in rice. *Plant and Cell Physiology*, 59:5. Pp. 903–915. <https://doi.org/10.1093/pcp/pcy062>
- Kröner A, Hamelin G, Andrivon D, Val F (2011) Quantitative Resistance of Potato to *Pectobacterium atrosepticum* and *Phytophthora infestans*: Integrating PAMP-Triggered Response and Pathogen Growth. *PLoS ONE* 6(8): e23331. <https://doi.org/10.1371/journal.pone.0023331>
- Li Y, Kim JI, Pysh L, Chapple C (2015) Four isoforms of *Arabidopsis* 4-Coumarate:CoA Ligase have overlapping yet distinct roles in phenylpropanoid metabolism. *Plant Physiology* 169 (4) 2409-2421; DOI: 10.1104/pp.15.00838
- Lorimer SD, Perry NB (1994) Antifungal hydroxy-acetophenones from the New Zealand liverwort, *Plagiochila fasciculata*. *Planta Med.* 60(4):386-7.
- Mhlongo MI, Steenkamp PA, Piater LA, Madala NE and Dubery IA (2016) Profiling of altered metabolomic states in *Nicotiana tabacum* cells induced by priming agents. *Front. Plant Sci.* 7:1527. doi: 10.3389/fpls.2016.01527

- Mock NM, Baker CJ, Aver'yanov AA (2015) Induction of a viable but not culturable (VBNC) state in some *Pseudomonas syringae* pathovars upon exposure to oxidation of an apoplastic phenolic, acetosyringone. *Physiol.Mol.PlantPathol.* 89,16–24.doi:10.1016/j.pmpp.2014. 11.006
- Negrel J, Javelle F, Wipf D (2014) Detection of an O-methyltransferase synthesising acetosyringone in methyl jasmonate-treated tobacco cell-suspensions cultures. *Phytochemistry* 99 52–60
- Newman MA, Sundelin T, Nielsen JT and Erbs G (2013) MAMP (microbe-associated molecular pattern) triggered immunity in plants. *Front. Plant Sci.* 4:139. doi: 10.3389/fpls.2013.00139
- Newman MA, von Roepenack-Lahaye E, Parr A, Daniels MJ, Dow JM (2001) Induction of hydroxycinnamoyl-tyramine conjugates in pepper by *Xanthomonas campestris*, a plant defense response activated by hrp gene-dependent and hrp gene-independent mechanisms. *Mol Plant Microbe Interact* 14: 785–792
- O'Brien JA, Daudi A, Finch P, Butt VS, Whitelegge JP, Souda P, FM Ausubel, GP Bolwell (2012) A peroxidase-dependent apoplastic oxidative burst in cultured *Arabidopsis* cells functions in MAMP-elicited defense. *Plant Physiology* 158 (4) 2013-2027; DOI: 10.1104/pp.111.190140
- Ramegowda V, Senthil-kumar M, Udayakumar M, Mysore KS (2013) A high-throughput virus-induced gene silencing protocol identifies genes involved in multi-stress tolerance. *BMC Plant Biology*, 13:1 p. 1
- Schillmiller AL, Stout J, Weng JK, Humphreys J, Ruegger MO, Chapple C. (2009) Mutations in the cinnamate 4-hydroxylase gene impact metabolism, growth and development in *Arabidopsis*. *Plant J.* 60(5):771-82. doi: 10.1111/j.1365-313X.2009.03996.x.
- Shakya R, Navarre DA (2006) Rapid screening of ascorbic acid, glycoalkaloids, and phenolics in potato using high-performance liquid chromatography. *Journal of Agricultural and Food Chemistry* 54 (15), 5253-5260 DOI: 10.1021/jf0605300
- Shinya T, Gális I, Narisawa T, Sasaki M, Fukuda H, Matsuoka H, Saito M, Matsuoka K (2007) Comprehensive analysis of glucan elicitor-regulated gene expression in tobacco BY-2 cells reveals a novel MYB transcription factor involved in the regulation of phenylpropanoid metabolism. *Plant & cell physiology.* 48(10). 1404-13.
- Stachel SE, Messens E, Van Montagu M, Zambryski P (1985) Identification of the signal molecules produced by wounded plant cells that activate T-DNA transfer in *Agrobacterium tumefaciens*. *Nature* 318:624-629.
- Sugimoto K, Takeda S, Hirochika H (2000) MYB-related transcription factor NtMYB2 induced by wounding and elicitors is a regulator of the tobacco retrotransposon Tto1 and defense-related genes *Plant Cell.*, 12, pp. 2511-2527
- Szabó E, Szatmári Á, Hunyadi-Gulyás É, Besenyei E, Zsiros LR, Bozsó Z, Ott PG (2012) Changes in apoplast protein pattern suggest an early role of cell wall structure remodelling in flagellin-triggered basal immunity. *Biologia Plantarum* 56:551-559. doi:10.1007/s10535-011-0226-0
- Szatmari A, Zvara A, Moricz AM, Besenyei E, Szabo E, Ott PG, Puskas LG, Bozso Z (2014) Pattern Triggered Immunity (PTI) in tobacco: Isolation of activated genes suggests role of the phenylpropanoid pathway in inhibition of bacterial pathogens. *PLoS ONE* 9(8), e102869
- Withers J, Dong X (2017) Post-translational regulation of plant immunity. *Curr Opin Plant Biol.* 38: 124-132. <https://doi.org/10.1016/j.pbi.2017.05.004>
- Xu XQ, Pan SQ. (2000) An *Agrobacterium* catalase is a virulence factor involved in tumorigenesis. *Mol Microbiol.*35(2):407-14.

Zhao Q, Dixon RA (2011) *Transcriptional networks for lignin biosynthesis: more complex than we thought?* *Trends in Plant Science* 16: 4, 227-233 <https://doi.org/10.1016/j.tplants.2010.12.005>